JIMMA UNIVERSITY

SCHOOL OF GRADUATE STUDIES

PREDICTION OF LONG-TERM SERVICEABLITY BEHAVIOUR OF A PRESTRESSED BOX-GIRDER BRIDGE UNDER A FATIGUE ACTION

A CASE STUDY ON AWASH BRIDGE

BY CHIMDI GADAFA

OCTOBER 2016

JIMMA ETHIOPIA

PREDICTION OF LONG-TERM SERVICEABLITY BEHAVIOUR OF A PRESTRESSED BOX-GIRDER BRIDGE UNDER A FATIGUE ACTION

A CASE STUDY ON AWASH BRIDGE

BY CHIMDI GADAFA

A THESIS SUBMITTED TO SCHOOL OF GRADUATE STUDIES OF JIMMA UNIVERSITY IN PARTIAL FULFILLMENT OF THE REQUIREMENT FOR THE DEGREE OF MASTER OF SCIENCE IN CIVIL ENGINEERING.

MAIN ADVISOR: Dr.Ing. ABRHAM GEBRE

CO-ADVISOR: Eng. AKLILU TADESSE

JIMMA UNIVERSITY

JIMMA EHIOPIA

OCTOBER 2016

Declaration

I declare that this thesis entitled ***"prediction of long-term serviceability behavior of a prestressed BOX girder bridge under fatigue action. A case study on AWASH bridge"*** is my original work. The work has not been presented by any other person in any other University and all sources of materials used for this thesis have been duly acknowledged.

<u>By Chimdi Gadafa</u>   _____   _____

     Researcher   *Signature*   *Date*

Approved by Board of Examiners

<u>Dr. Abrham Gebre</u>   _____   _____

    (Main Advisor)   *Signature*   *Date*

<u>Mr. Aklilu Tadesse</u>   _____   _____

    (Co- Advisor)   *Signature*   *Date*

<u>Dr. Temesgen Wondimu</u>   _____   _____

    (External Examiner)   *Signature*   *Date*

_____   _____   _____

    (Internal Examiner)   *Signature*   *Date*

_____   _____   _____

    (Internal Examiner)   *Signature*   *Date*

Abstract

In bridge design, engineers strive to plan an economical structure that will safely transmit loads to the ground without collapsing or deforming excessively. Since it is difficult to predict the exact loading and circumstances that a bridge must withstand, all bridge designs include a substantial margin of safety. Design standards vary throughout the world, but all aim at ensuring that constructed bridges will provide many years of service and will maintain an adequate margin of safety against failure.

Bridges are mainly faced to the problem of fatigue from cyclic loading condition which in turn affects the future serviceability and performance of bridge. The future service ability related behavior of bridge includes loss of internal stresses, deflection and crack.

PSC Bridges of longer span often exhibit larger long-term serviceability related problems than it was assumed in the design calculation. The future serviceability and performance check for PSC Bridge involves a number of steps which involves tedious and complex calculations due to the presence of variable moving loads and other environmental factors applied over service life of bridge.

In line with this, this thesis is focused on prediction of long term serviceability behavior of a prestressed AWASH Bridge under a fatigue action starting from opening of traffic (December 2014) to the end of 2030. In this case the problem is only for long term behavior of un-cracked girder under fatigue action during its operational period. The prediction is done using MATLAB, and MATHCAD PRIME spread sheet and it is shown on appendix.

Key words: Deflection, Fatigue, Girder, Losses, Prestressing, Serviceability,

Acknowledgements

Table of Contents

List of tables

List of figures

Abbreviation and Symbols

AADT: Average Annual Daily traffic

AASHTO: American Association of State of Highway and Transportation Officials

ACI: American Concrete Institute

ADT: Average Daily Traffic

BMD: Bending Moment Diagram

CESAL: Cumulative Equivalent Standard Axle Load

CR: Creep of concrete

EALF: Equivalent Axle Load Factor

EPt: Effective Prestressing force at time t

ERA: Ethiopian Road Authority

ESAL: Equivalent Standard Axle Load

ESWL: Equivalent Single wheel load

IPL: Instantaneous Prestress losses

LFRD: Load Resistance Factored Design

LPLt: Long term Prestress Loss at time t

LPt: Long term loss in prestressing force at time t

LPin: Instantaneous Loss in prestressing force

NCDOT: North Carolina Department of Transportation

NCHRP: National Cooperative Highway Research Program

PCI: Prestressed Concrete Institute

PSC: Prestressed Concrete

RE: Relaxation of steel

SR: Shrinkage of concrete

TPLt: Total Prestress Loss a time t

TLPT: Total Loss in prestressing force at time t

TF: Truck Factor

WIM: Weight in Motion

A: Cross sectional area of girder

Ac: Cross-sectional area of the net concrete section of girder

A_{ps}: Total cross-sectional area of the pre stressing steel

$\overline{A_t}$: Cross-sectional area of the age-adjusted transformed girder section

A_t: Cross-sectional area of the initial transformed girder section

e: Eccentricity of tendon from the centroid

e_m: Eccentricity at mid span with respect to the centroid of the gross section

e_e: Eccentricity at the end of the girder with respect to the centroid

EI : Flexural rigidity of the girder

$\overline{e}_{np}$: Eccentricity with respect to centroid of the age-adjusted transformed section

$E_c(t_i)$: Modulus of elasticity of concrete at the time of post-tensioning

E_{ci}: Elastic modulus of the concrete at transfer

$\overline{E_c}(t,t_i)$: Age-adjusted modulus of elasticity of concrete between time t and t_i

E_s: modulus of elasticity of the prestressing steel

f_{cgp}: Concrete stress at center of gravity of prestressing steel at transfer

f_{pi}: Initial stress in the prestressing steel

f_{py} : Yield strength of the prestressing steel

g: self-weight of the girder

h: Depth of girder

Ic : Moment of inertia of the net concrete section of girder

I_g: Moment of inertia of the gross section

$\overline{I_t}$: Moment of inertia of the age-adjusted transformed girder section

I_t: Moment of inertia of the initial transformed girder section

L: Length of girder

Mq: Live load moments

Mg: Dead load moments

M_{total}: Total moment at the girder section right after post-tensioning

P: Effective pre stressing force

P_i: Initial pre stress

P_t: Pre stress after time t

q: live load on the girder

$t_i =$ Age of concrete at the time of post-tensioning

t: Time (days) between stressing and transfer

w_{sd}: Linearly distributed live load applied at bridge erection

W_g: Linearly distributed self-weight load

Z_t: Section modulus of top fibers

Z_b: Section modulus of bottom fibers

Δf_{pED} : Instantaneous prestress gain due to the placement of deck weight

Δf_{pES}: Loss due to elastic shortening

$\Delta f_{pc}(t,t_i)$: Creep loss between time instants t and t_i

Δf_{pCR}: Loss due to concrete creep

$(\Delta f_{pCR})_{id}$: Loss due to creep between the time of transfer and before deck placement.

$\Delta f_{PR}(t,t_i)$: Relaxation loss of prestressing steel between time instants t and t_i

Δf_{R2} : Loss due steel relaxation

$(\Delta f_{pR2})_{id}$: Loss by relaxation between the time of transfer and before deck placement.

$\Delta f_{ps}(t,t_i)$: Shrinkage loss between time instants t and t_i

Δf_{pSR}: Loss due to concrete shrinkage

$(\Delta f_{pSR})_{id}$: Shrinkage loss between the time of transfer and before deck placement.

$\Delta_{ps,i}$: Upward deflection due to pre stressing

Δ_{sd} : Deflection due to live load applied at bridge erection

$\Delta_{sw,i}$: Downward deflection due to girder self-weight

$\Delta\sigma_{p0}$: Stress in the strand after jacking

$\Delta\sigma_{pr}$: Reduction in stress is known as intrinsic relaxation

Δy : Distance of the centroid of the age-adjusted section from net concrete section

σ_t : Total stress at the top

σ_b : Total stress at bottom

$\varepsilon_{free}(t,t_i)$: Free strain between time instants t and t_i

$\varepsilon_o(t_i)$: Instantaneous strain at t_i

$\varepsilon_{sh}(t,t_i)$: Shrinkage strain between time instants t and t_i

$\bar{\varepsilon}_{cp}(t,ti)$: Creep strain of concrete at the centroid of the pre stressing steel.

ϕ_i : Initial curvature

ϕ_{mt}: Change of curvature caused by transverse load

ϕ_{pt} : Change of curvature caused by pre stress

ϕ_t: Net curvature

$\phi_{free}(t,t_i)$: Free curvature between time instants t and t_i

$\phi(t_i)$: Instantaneous curvature at t_i

$\phi(t,t_o)$: Ratio of the creep strain to the instantaneous strain

χ : Time averaging factor

α_{ps} : Modulus ratio

Δdt: Down ward deflection by gravity load at time t

Δnt: Net deflection of a bridge at time t

Δut: Upward ward deflection by effective prestressing force at time t

CHAPTER ONE-INTRODUCTION

1.1.   Back ground of the study

Bridge construction in Ethiopia was early started on Blue Nile near Alata, Almeida Bridge placed across the narrow rocky banks. During the period following Fassiledes (after 1667) it is said that many bridges were constructed in Gonder and Lake Tana area.

In Addis Ababa, the first bridge was constructed on Kebena River in 1902 by a Russian engineer after their compatriot was drowned. The second was Ras Mekonnen Bridge, arch type bridge, in 1908. Quite considerable numbers of bridges were constructed in the years 1935-1945, the years of occupations by Italians. Notable bridges have been constructed since 1970's. *(Abrham G, 2006)*

Slab and T- Girder bridges made using reinforced concrete, mostly with simple supports but either single span or spans in series are the most commonly used bridges in Ethiopia.

Now a day PSC technology is under consideration for longer spans and different purposes using higher concrete strength. Prestressing (pre and post-tensioning) is the creation within a material of a state of stress and strain that will enable it to better perform its intended function.

About 1890, Henry Jackson, a San Francisco engineer, reportedly develops a PSC technology. The world's first prestressed concrete bridge was built in Aue, Germany in 1937 using Dischinger's system. In spite of careful design and construction, the bridge was unsuccessful after 25 years, losing 75% of its initial prestress through creep and shrinkage. Modern development of prestressed concrete is credited to E. Freyssnet of France, started in 1928 using high-strength steel wires and concrete for PSC

In Ethiopia there were different PSC technologies, i.e. Abay River Bridge constructed in 1983 over Abay River on the route from Bure to Nekemte towns. The main part of the bridge is composed of a three continuous spans, 85 meter central span and 52 meter end spans totally 189 meters overall length. The bridge has got two lanes with sidewalk ways.

The cross-section of the bridge is single cell box with flares at each corner. *(Tewodros T, 2009)*
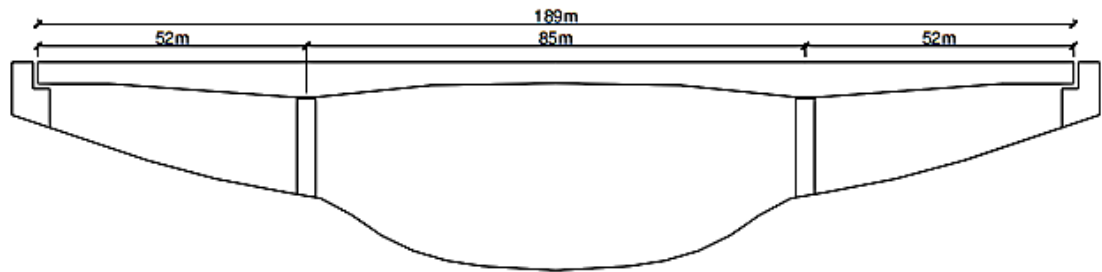
Fig.1.1. Longitudinal section of Abay River Bridge (1983)

South Awash River Bridge is constructed in March 1966 over Awash River on the road from Awash to Mille Towns at around 5.4 km from Awash town. The bridge is composed of three spans consisting 67 meters central span and two 21 meters side spans totally 109 meters overall length as shown in fig below. And also it is composed of box, T, and I girders at different sections longitudinally. *(Tewodros T, 2009)*
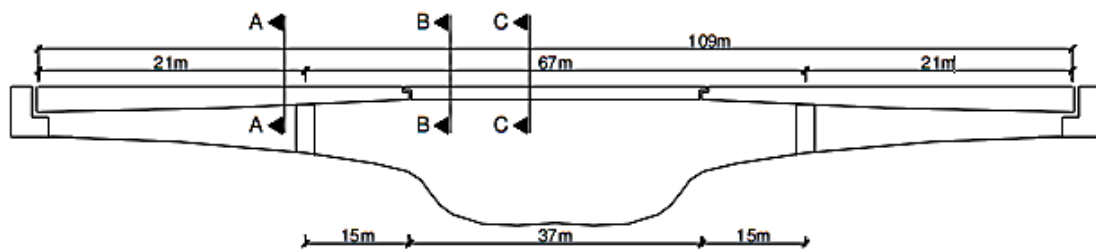
Fig.1.2. Longitudinal section of Awash River Bridge (1966)

Recently this PSC technology is well practiced and ongoing in Ethiopia. A new alternative PSC bridge over Awash River along Ethio- Djibouti with span length of 145 meters is constructed and opened to traffic on December 2014.
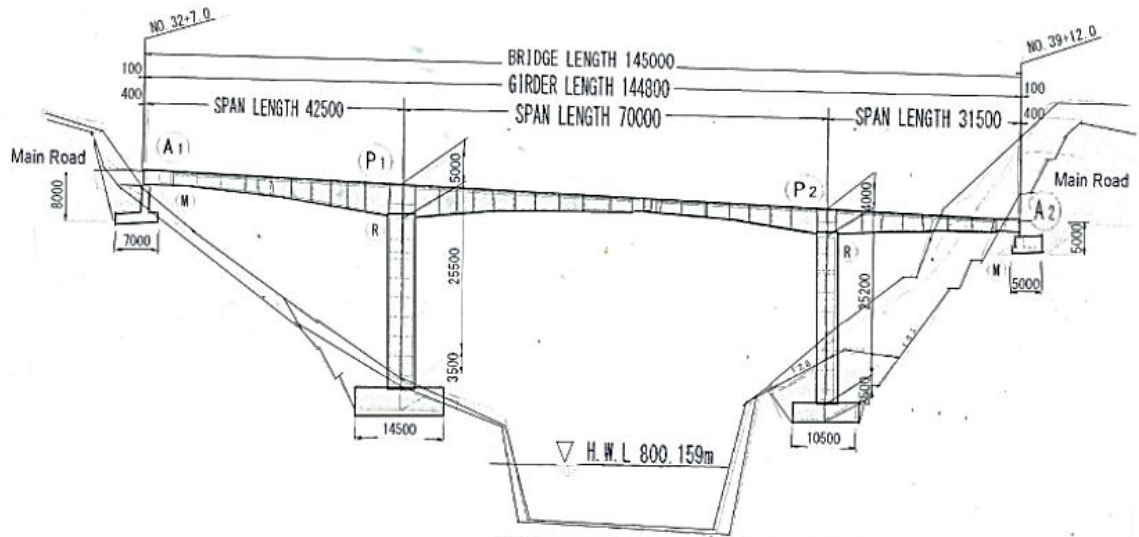
Fig.1.3. Longitudinal section of alternative Awash River Bridge (2014)

1.2. Statement of the problem

The actual tendency in civil engineering is to extend the life-cycle of large scale structures. Designing with redundancy against structural failure increases the overall safety of the bridge. Any numerical results produced by engineering software need to be checked for consistency and accuracy of results to capture errors or omissions that might have been incurred during the modeling process. Finally, the results need to be interpreted by the structural engineer to apply them to the real structure.

For PSC Bridge we should have to pay attention while analysis, design and construction to increase service life of bridge and to minimize maintenance cost during its operational period. Serviceability behavior of PSC Bridge is affected by Environmental factors and fatigue action to be applied over service life of bridge.

Realistically, prediction of the long-term behavior of a long-span prestressed concrete bridge is a serious challenge to the current progress towards sustainable transportation system, which requires for a longer service lifetime. According to a recent survey (Bazant et al., 2012), a great number of bridges worldwide are suffering the excessive deflections which were significantly underestimated in design. Unexpected deflection will result in cracks in concrete members, and therefore significantly compromise the safety and serviceability of a prestressed concrete bridge.

For example, the Koror-Babeldaob (KB) Bridge with a large-span of 241m developed an excessive deflection and collapsed in 1996.

Here the main issue under consideration in this thesis is effect of fatigue or cyclic load on the performance, capacity and service ability behavior of prestressed AWASH Bridge during its operational period. Long term behavior of the bridge includes prediction of prestress losses and deflection under fatigue action and time.

Serviceability related behavior of PSC Bridge affected by:

- Initial analysis, design and construction method
- Magnitude of prestressing force
- Fatigue action/ cyclic traffic load
- Time /inverse to serviceability
- Environmental factors (temperature, humidity...)

Serviceability related behaviors of PSC Bridge under fatigue action & time constraint.

- Long-term deflection : before and after crack
- Growth of crack
- Loss of internal stresses : Immediate and Time dependent

In this thesis serviceability behaviors predicted include the 1st and 3rd parameters.

1.3. Research Questions

The research will be mainly focuses to answer the following research questions:

- What is the need of prediction for long- term serviceability behavior of PSC Bridge?
- What are PSC related main aims of this research?
- What are factors affecting long term serviceability of PSC Bridge?

1.4. Obtained Outcomes

From this research:

- ➢ Prediction for prestress losses of the AWASH Bridge under fatigue load and time.
- ➢ Prediction for long-term deflection of AWASH Bridge under fatigue load and time.

1.5. Objectives of the Study

1.5.1. General Objective

The main aim of this research is prediction of long term serviceability behavior of PSC box-girder Bridge under fatigue action of traffic load.

1.5.2. Specific Objectives

Specifically thesis research has the following objectives:

- ➢ To calculate time dependent prestress losses of PSC girder bridge under fatigue load using computer program
- ➢ To calculate long term deflection of PSC girder bridge under fatigue load
- ➢ To determine factors affecting long term serviceability of PSC Girder Bridge.

1.6. Limitations of the Study

This research is limited to:
- ➢ PSC Bridge under fatigue / traffic loading condition
- ➢ PSC Bridge with no visible crack
- ➢ PSC Bridge for High way asset
- ➢ Prediction of long term prestress losses and deflection for PSC Bridge

CHAPTER TWO- LITRATURE RIVIEW

2.1. Introduction to Fatigue Action

It is a known fact that if the maximum load acting on a structure becomes higher than its material yield strength limit, a failure is assumed in the structure. However, in a structure that undergoes fluctuating loads, even if they have low elastic limit of material, a failure can be expected after many loading cycles. The later situation, which is a result of accumulated damages in the material, is known as fatigue failure. In other words, static loading of a ductile material which increases from zero to a maximum, will cause large deformations. In that case, failure of the structure occurs after a single load application with large plastic deformation, whereas, if the same material is repeatedly loaded to stresses well below the elastic limit, fatigue failure may happen after as little as a few hundred cycles or after, say, several million cycles of load application without any large plastic deformation. However, it should be noted that fatigue can happen not only in metallic alloys but also in a large number of engineering materials such as polymers and composites, e.g. concrete and fiber reinforced plastics.

Fatigue is the process of progressive localized permanent structural change occurring in a material subjected to conditions that produce fluctuating stresses and strains at some point or points and that may culminate in cracks or complete fracture after a sufficient number of fluctuations. Therefore, the process of fatigue is time consuming and can only happen as an outcome of a repeated loading. In most cases the crack initiates in a confined small area that is either subjected to high local stresses or suffering from local defects in the material. On the contrary, in adjacent parts, where the stress state is insignificantly lower, no crack would initiate. Hence, fatigue is clearly a much localized process in which the crack originates in a location where several micro cracks are available and grow together into one dominant crack. The mentioned process of crack formation after a coalescence of several micro-cracks is called the initiation phase of fatigue crack growth and is a result of plastic deformations in a small area in front of the crack tip. The presence of plastic deformations also implies that fatigue is an irreversible process which leaves permanent structural damages. *(Mohsen H, 2012.)*

2.2. Prediction of prestress losses

2.2.1. Introduction

A prestressed girder member supports uniformly distributed live load q (positive when produce direct compression) and dead load g (positive when produce direct compression). The girder is prestressed by a tendon carrying a prestressing force of P (positive when produce direct compression) at an eccentricity e. The resultant stress in concrete at any section is obtained by super imposing the effects of prestress and flexural stress developed due to the loads. *(N Krishna R. Prestressed concrete structures, 4th edition.)*
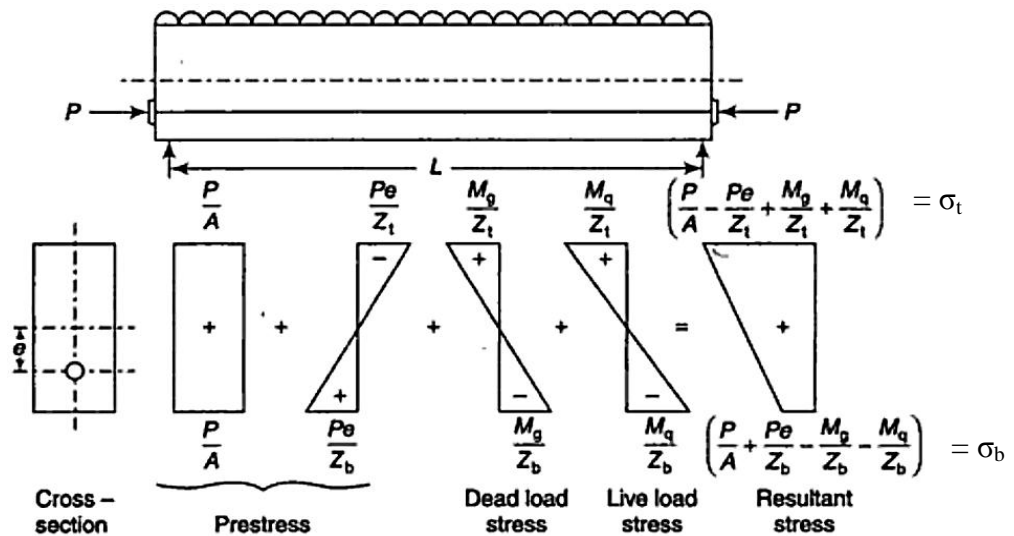
Fig.2.1. Stress distribution due to eccentric prestressing, live and dead load

Where:

σ_t and σ_b total stress at the top and bottom respectively

Z_t and Z_b section modulus of top and bottom fibers respectively

A cross sectional area

Mq and Mg are the live and dead load moments respectively

The prestress losses are broadly classified into two groups, immediate and time-dependent. The immediate losses occur during prestressing of the tendons and the transfer of prestress to the concrete member. The time dependent losses occur during the service life of the prestressed member.
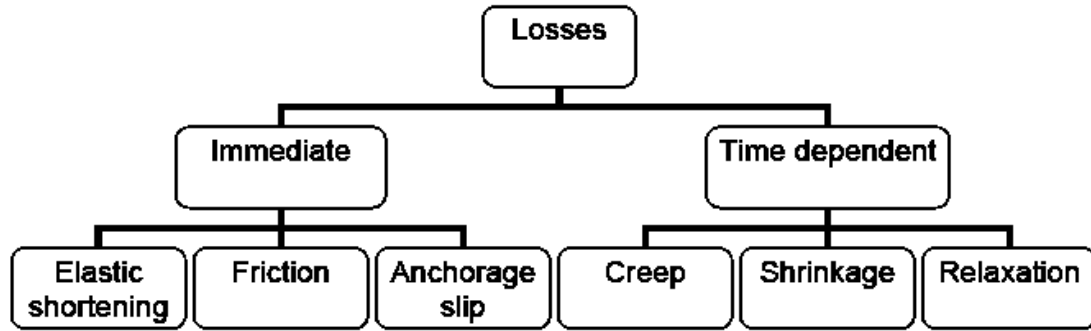
Fig.2.2. Types of prestress losses

Table 2.1 losses encountered in pre-tensioning and post-tensioning system

No	Pre-tensioning	No	Post-tensioning
1	Elastic deformation of concrete	1	Elastic deformation of concrete (wires are tensioned successively)
2	Relaxation of stress in steel	2	Relaxation of stress in steel
3	Shrinkage of concrete	3	Shrinkage of concrete
4	Creep of concrete	4	Creep of concrete
		5	Friction
		6	Anchorage slip

Accurate prediction of the long-term prestress losses in concrete bridge girders is an important part of the design process. An over prediction in the prestress loss could mean a limitation of the span length of the girder, and a considerable increase in the prestressing force required to overcome such losses. On the other hand, an under-prediction of the prestress losses could translate into undesired deflections and cracking under service conditions. Because in many concrete bridge girders, the cracking control under service loads is the controlling parameter in the design process, a precise but safe prestress loss prediction method is imperative. Prestress losses can be defined as the decrease in the initial prestressing force. There are two main types of prestress losses depending on the time and duration of their occurrence; the first is the instantaneous elastic shortening loss. The second type is the long-term losses, mostly due to relaxation

of the pre stressing strands and creep and shrinkage of the concrete. Prestress losses are also influenced by other time-dependent concrete properties, like its compressive strength and its modulus of elasticity. *(Franklin B, 2009.)*

2.2.2. Prediction of prestress losses: N Krishna R

The initial prestress in concrete under goes a gradual reduction with time from the stage of transfer due to various causes. This is gradually referred to as loss of prestress. A reasonable good estimate of the magnitude of loss of prestress is necessary from the point of view of design.

1. Loss due to elastic shortening

Elastic shortening losses are easily determined by applying the prestressing force at the time of release (the jacking force minus the appropriate amount of steel relaxation) to the transformed girder section. The loss of prestress due to elastic deformation of concrete depends on the modular ratio and average stress in concrete at the level of steel.

If, f_c = stress in concrete at the level of steel

E_s = modulus of elasticity of steel E_c = modulus of elasticity of concrete

$$\alpha_c = \frac{E_s}{E_c} = \text{Modular ratio}$$

Loss of stress in steel becomes = $\alpha_c f_c$

2. Loss due to shrinkage of concrete

The shrinkage of concrete in prestressed girder is due to the gradual loss of moisture which results in change in volume.

The shrinkage of concrete in pre stressed member results in shortening of tensioned wires and hence contributes to the loss of stress. The shrinkage of concrete is influenced by the type of cement, aggregates, water/cement ratio in the mix, the time of exposure and the method of curing and degree of hardening used. Use of high strength concrete with low water cement ratios results in reduction of in shrinkage and consequent loss of prestress. The primary cause of drying shrinkage is the progressive loss of water from concrete.

The rate of shrinkage is higher at the surface of the members. The differential shrinkage between the interior and surface of large members may result in strain gradients leading to the surface to surface cracking. Hence, proper curing is essential to prevent shrinkage cracks in prestressed members.in the case of pre-tensioned girders, generally moist curing is resorted in order to prevent shrinkage until the time of transfer. Consequently, the total residual shrinkage strain is larger in pretensioned girder after transfer of prestress in comparison with post-tensioned girder.

ε_{cs} = total residual shrinkage strain

$= 300*10^{-6}$ for pre-tensioned girder

$= \dfrac{200*10^{-6}}{\log_{10}(t+2)}$ for post- tensioned girder, t is age of concrete at transfer in days

The loss of stress in steel becomes $= \varepsilon_{cs}E_s$, where E_s is modulus of elasticity of steel

3. *Loss due to creep of concrete*

The sustained prestress in the concrete of prestressed girder results in creep of concrete which effectively reduces the stress in high tensile steel. The progressive inelastic strains due to creep in a PSC girders are likely to occur under the smallest sustained stresses at ambient temperatures. Shrinkage and creep of PSC are similar in origin. For the design purpose it is convenient to differentiate the deformation due to externally applied stress, generally referred to as creep, and the deformation which occurs without externally applied stress, referred to as shrinkage. The various factor influencing creep of PSC are relative humidity, stress level, strength of concrete, age of concrete at loading, duration of stress, water/cement ratio, type of cement and aggregate.

The loss of stress in steel due to creep of concrete can be estimated if the magnitude of ultimate creep strain or creep coefficient is known.

A) Ultimate creep strain method

If ε_{cc} = ultimate creep strain for sustained unit stress

f_c = stress in concrete at the level of steel

E_s = is modulus of elasticity of steel

Then the loss of stress in concrete becomes = $\varepsilon_{cc} f_c E_s$

Ultimate creep strain is $48*10^{-6}$ for pre-tensioning and $36*10^{-6}$ for post- tensioning

B) Creep coefficient method

If ϕ= creep coefficient, α_c = modular ratio

ε_c= creep strain f_c = stress in concrete at the level of steel

ε_e = elastic strain E_s = is modulus elasticity of steel

E_c= is modulus of elasticity of concrete

$$\phi = \frac{\varepsilon_c}{\varepsilon_e} \Rightarrow \varepsilon_c = \phi\varepsilon_e \Rightarrow \phi(\frac{f_c}{E_c})$$

Then the loss of stress in concrete becomes = $\varepsilon_c E_s \Rightarrow \phi(\frac{f_c}{E_c})E_s \Rightarrow \phi f_c E_s$

The magnitude of creep coefficient varies based on humidity, concrete quality, duration of applied load and age of concrete. The general values recommended for creep coefficient vary from 1.5 for watery situation to 4.0 for dry conditions under relative humidity of 35%

4. Loss due to friction

In the case of post-tensioned members, the tendons are housed in ducts performed in concrete. The ducts are either straight or follow a curved profile depending on the design requirements. Consequently, on tensioning the curved tendons, loss of stress occurs in the post-tensioned girders due to friction between the tendons and the surrounding concrete ducts. The magnitude of this loss is of the following types:

a) Loss of stress to the curve effect, which depends upon the tendon form or alignment which generally follows a curved profile along the length of the beam.

b) Loss of stress due to the wobble effect, which depends upon the local deviations in the alignment of the cable. The wobble or wave effect is the result of accidental or unavoidable misalignment, since ducts or sheath cannot be perfectly located to follow a predetermined profile throughout the length of the beam

The following figure shows that the magnitude of prestressing force P_x at distance x from the tensioned end in exponential function.

$$P_x = P_o e^{-(\mu\alpha+kx)}$$
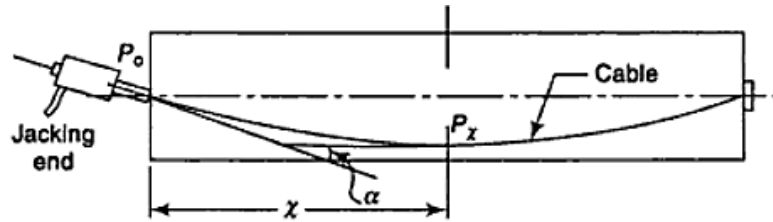
Fig2.3. loss of stress due to friction

Where, P_o = prestressing force at the end of the jacking end

     μ = coefficient of friction between cable and duct

     α = the cumulative angle in radian through which the tangent to the cable profile

        has turned between any two points under consideration

     K = friction coefficient for wave effect

     e = 2.7183

     μ = 0.55 for steel moving on smooth concrete

        = 0.35 for steel moving on steel fixed to duct

        = 0.25 for steel moving on steel fixed to concrete and steel moving on lead

     K = 0.15 per 100m for normal condition

        = 1.5 per 100m for thin walled ducts

        = reduced to zero where the clearance between duct and cable is large

5. *Loss due to anchorage slip*

In most post-tensioning of PSC systems, when the cable is tensioned and the jack is released to transfer prestress to concrete, the friction wedges, employed to grip the wires, slip over a small distance before the wires are firmly housed between wedges. The magnitude of slip depends upon the types of wedge and the stress in the wires. The magnitude of loss of stress due to slip in anchorage is computed as follows.

If Δ = slip of anchorage, mm

    L = length of cable, mm

    A_p = cross sectional area of cable, mm^2

    E_s = modulus of elasticity of steel. N/mm^2

    P = prestressing force in the cable, N then

$$\Delta = \frac{PL}{A_p E_s} \text{ and the loss of stress in concrete becomes:}$$

$$\text{Asl} = \frac{P}{A_p} = \frac{\Delta E_s}{L}$$

2.2.3. Long term prestress losses: Youakim and Karbhari

1. Prediction of losses due to creep and shrinkage

The total creep and shrinkage loss between time instants *t* and t_i is given by the following equation.

$$\Delta f_{pc}(t,t_i) + \Delta f_{ps}(t,t_i) = E_s \{ k_A \varepsilon_{free}(t,t_i) - e[k_I \phi_{free}(t,t_i) + \frac{k_h \varepsilon_{free}(t,t_i)}{h}]\}$$

Where, E_s = modulus of elasticity of the prestressing steel

    e = eccentricity of the prestressing force with respect to the centroid of the age-adjusted transformed girder section; positive when the prestressing force is below the centroid of the section

    h= depth of girder

    t_i = age of concrete at the time of post-tensioning

$$k_A = \frac{A_c}{\overline{A_t}}, k_I = \frac{I_c}{\overline{I_t}}, k_h = \frac{A_c \Delta yh}{\overline{I_t}}, with$$

    Δy =distance of the centroid of the age-adjusted transformed girder section from that of the net concrete section; positive if the former is below the later

    Ac, Ic = cross-sectional area and moment of inertia of the net concrete section

    $\overline{A_t}, \overline{I_t}$ = cross-sectional area and moment of inertia of the age-adjusted transformed girder section, which includes the prestressing steel and mild

reinforcement, and the transformed section is based on the age-adjusted modulus of elasticity of concrete, $\overline{E_c}(t,t_i)$

The age-adjusted modulus of elasticity of concrete is defined as: $\overline{E_c}(t,t_i) = \dfrac{E_{ci}}{1 + \chi\psi(t,t_i)}$

where $E_{ci} = E_c(t_i)$, the modulus of elasticity of concrete at the time of post-tensioning, and χ is a time averaging factor, whose value is recommended by Youakim and Karbhari to be 0.8. In AASHTO 2007, the time averaging factor is assumed to be 0.7 for the refined analysis method. Since the difference between the two recommended values is very small, the value of 0.7 is adopted for all the prestress loss calculations conducted in this study to be consistent with the AASHTO specifications.

The free strain and free curvature are computed with the following equations. It should be noted that curvature is considered positive when it is concave upward.

$$\varepsilon_{free}(t,t_i) = \psi(t,t_i)[\varepsilon_o(t_i) - \phi(t_i)\Delta y_l] + \varepsilon_{sh}(t,t_i)$$
$$\phi_{free}(t,t_i) = \psi(t,t_i)\phi(t_i)$$

Where, Δy_l is the distance of the centroid of the net concrete section from that of the initial transformed girder section (positive if the former is below the later), which is defined below. The value of Δy_l is normally very small so that it can be assumed zero. The shrinkage strain is defined as $\varepsilon_{sh}(t,t_i) = \varepsilon_{sh}(t) - \varepsilon_{sh}(t_i)$. The instantaneous strain $\varepsilon_o(t_i)$ at the centroid of the initial transformed section of the girder and the instantaneous curvature $\phi(t_i)$ can be computed as:

$$\varepsilon_o(t_i) = \frac{A_{ps}f_{pi}}{E_{ci}A_t}, \text{ and } \phi(t_i) = \frac{M_{total}}{E_{ci}I_t}, \text{ where}$$

A_{ps} = total cross-sectional area of the pre stressing steel

f_{pi} = initial stress in the pre stressing steel right after post-tensioning

M_{total} = total moment at the girder section right after post-tensioning.

   It is usually the sum of the moments induced by the self-weight and the equivalent load of the prestressing force

A_t, I_t = cross-sectional area and moment of inertia of the initial transformed girder section, which includes the net concrete section and mild reinforcement but excludes the prestressing steel; the transformed section is based on the elastic modulus of concrete, E_{ci}, at the time of post-tensioning

To separate the respective contributions of creep and shrinkage, equation can be divided into the following two expressions with Δy_l assumed to be zero.

$$\Delta f_{pc}(t,t_i) = E_s \psi(t,t_i)\{k_A \varepsilon_o(t_i) - e[k_I \phi(t_i) + \frac{k_h \varepsilon_o(t_i)}{h}]\}$$

$$\Delta f_{ps}(t,t_i) = E_s\{k_A \varepsilon_{sh}(t,t_i) - e[\frac{k_h \varepsilon_{sh}(t,t_i)}{h}]\}$$

2. Prediction of relaxation loss

The following expression is used to calculate the relaxation loss of the prestressing steel.

$$\Delta f_{PR}(t,t_i) = \chi_r \Delta \overline{f}_{PR}(t,t_i)[1 - \frac{E_S)}{\overline{E}_c(t,t_i)}(k_{AP} + k_y)]$$

With the value of χ_r recommended to be 0.7, which is to account for the influence of the creep and shrinkage losses on steel relaxation.

$$k_{AP} = \frac{A_{ps}}{\overline{A}_t} \; and, k_y = \frac{A_{ps}e^2}{\overline{I}_t} \qquad \Delta \overline{f}_{PR}(t,t_i) = \frac{\log(24)(t,t_i))}{K^{'}}\left(\frac{f_{pi}}{f_{py}} - 0.55\right)f_{pi}$$

Where, f_{py} is the yield strength of the prestressing steel and f_{pi} is the initial prestress in the steel. In the above expression, time is in days and t_i is the time at which the post-tensioning force is first applied.

$$\Delta f_{PR}(t,t_i) = 0.85 \chi_r \Delta \overline{f}_{PR}(t,t_i)$$

2.2.4. Long term prestress losses: Tadros

1. Creep and Shrinkage losses

In the following derivation, the prestressing force is treated as an external force applied to the girder section, which includes the net concrete section and mild reinforcement. Furthermore, with the assumption of no bond slip, the incremental strain in the prestressing steel must be equal to that in the concrete at the same elevation. The shrinkage strain that will be realized in a girder section with mild reinforcement can be calculated as $\varepsilon_{sh}(t,t_i)\dfrac{A_c}{A_n}$, where ε_{sh} is the unrestrained shrinkage strain of concrete, A_c is the net concrete area of the girder section, and A_n is the area of the age-adjusted transformed girder section consisting of concrete and mild reinforcement only. Hence, enforcing the incremental strain compatibility condition, we have:

$$\frac{\Delta f_{pS}}{E_p} = k'_A \varepsilon_{sh}(t,t_i) - \left(\frac{A_{ps}\Delta f_{pS}}{\overline{E_c}\,\overline{A}_n} + \frac{A_{ps}\Delta f_{pS}\,\overline{e}^{\,2}_{np}}{\overline{E_c}\,\overline{I}_n}\right)$$

Where $\overline{E_c}$: is the age adjusted modulus of elasticity of concrete

$$k'_A = \frac{A_c}{\overline{A}_n},$$

$\overline{A}_n, \overline{I}_n =$ cross-sectional area and moment of inertia of the age-adjusted transformed girder section, which includes the net concrete area and mild reinforcement, and the transformed section is based on the age-adjusted modulus of elasticity of concrete, $\overline{E_c}$

$\overline{e}_{np}$ = eccentricity of the prestressing force with respect to centroid of the age-adjusted transformed girder section; positive when the prestressing force is below the centroid of the section.

By rearranging and taking χ to be 0.7 as in the AASHTO 2007 Specifications, we have:

$$\Delta f_{pS}(t,t_i) = E_p k'_A \varepsilon_{sh}(t,t_i) K_{idn}$$

$$K_{idn} = \cfrac{1}{1 + \cfrac{E_p}{E_{ci}} \cfrac{A_{ps}}{\overline{A}_n}(1 + \cfrac{\overline{A}_n \overline{e}_{np}^{-2}}{\overline{I}_n})(1 + 0.7\psi(t,ti))}$$

With $E_{ci} = E_c(ti)$, the modulus of elasticity of concrete at the time when the prestressing force is first applied.

For calculating the prestress loss due to the creep of concrete, three scenarios are considered for the girder section. One is the initial transformed section, which consists of the net concrete area and mild reinforcement with the modulus of elasticity of concrete taken to be E_{ci}; the second is the net concrete section, which consists of concrete only; and the third is the age adjusted transformed section that includes the net concrete area and mild reinforcement and is calculated with the age-adjusted modulus of elasticity, E_c. The following expression is used for the creep strain of concrete at the location of the centroid of the prestressing steel.

$$\text{Where: } \overline{\varepsilon}_{cp}(t,t_i) = \overline{\varepsilon}_{co}(t,t_i) - \overline{e}_{np}\, \overline{\phi}(t,t_i)$$

$$\overline{\varepsilon}_{co}(t,t_i) = k'_A(\varepsilon_o(t_i) - \phi(t_i)\Delta_{yi})\psi(t,ti)$$

$$\overline{\phi}(t,t_i) = k'_I\phi(t_i)\psi(t,ti) + \frac{A_c}{\overline{I}_n}(\varepsilon_o(t_i) - \phi(t_i)\Delta_{yI})\psi(t,ti)\Delta_y$$

With $\varepsilon_o(ti)$ and $\phi(ti)$ being the instantaneous strain and curvature Δy_l being the distance of the centroid of the net concrete section from that of the initial transformed girder section (positive if the former is below the later), Δy being the distance of the centroid of the age-adjusted transformed section from that of the initial transformed girder section (positive if the former is below the later), $\overline{I}_n$ being the moment of inertia of the age adjusted transformed section, and $k'_I = \dfrac{I_c}{\overline{I}_n}$. It should be noted that A_c and I_c are the area and moment of inertia of the net concrete section. Assuming that Δy_l is zero, which is a good approximation, we have:

$$\overline{\varepsilon}_{cp}\,(t,t_i) = (k'_A - \frac{\overline{e}_{np}Ac\Delta y}{\overline{I}_n})\varepsilon_o\,(t_i)\psi(t,t_i) - k'_I\,\overline{e}_{np}\,\phi(t_i)\psi(t,t_i)$$

The incremental strain compatibility condition gives:

$$\frac{\Delta f_{pS}}{E_p} = \overline{\varepsilon}_{cp}\,(t,t_i) - (\frac{A_{ps}\Delta f_{pS}}{\overline{E}_c\overline{A}_n} + \frac{A_{ps}\Delta f_{pS}\overline{e}^2_{np}}{\overline{E}_c\overline{I}_n}$$

By substitution we have:

$$\Delta f_{pC}(t,t_i) = E_p[(k'_A - \frac{\overline{e}_{np}Ac\Delta y}{\overline{I}_n})\varepsilon_o\,(t_i) - k'_I\,\overline{e}_{np}\,\phi(t_i)]\psi(t,t_i)$$

Finally by substitution we have:

$$\Delta f_{pC}(t,t_i) = \frac{E_p}{E_{ci}}\mathrm{f}'_{cgp}\psi(t,t_i)K_{idn}$$

Where

$$\mathrm{f}'cgp = (k'_A - \frac{\overline{e}_{np}Ac\Delta y}{\overline{I}_n})\frac{A_{ps}f_{pi}}{A_t} - k'_I\,\overline{e}_{np}\,\frac{M_{total}}{I_t}$$

A_t and I_t are the area and moment of inertia of the initial transformed girder section not including the prestressing steel.

2. Relaxation loss

Considering the incremental strain compatibility condition, we have:

$$\frac{\chi_r\Delta\overline{f}_{pR} - \Delta f_{pR}}{E_p} = \frac{A_{ps}\Delta f_{pR}}{\overline{E}_c\overline{A}_n} + \frac{A_{ps}\Delta f_{pR}\overline{e}^2_{np}}{\overline{E}_c\overline{A}_n}$$

Where $\Delta\overline{f}_{PR}$ is given as Youakim and Karbhari's Method which is a widely accepted formula for calculating relaxation loss in prestressing strands subjected to a constant tensile strain, χ_r is a reduction factor to account for the gradual reduction of the tensile

strain in the prestressing strands over time due to the creep and shrinkage of concrete, A_{ps} and E_p are the total cross-sectional area and modulus of elasticity of the prestressing steel, and Δf_{PR} is the final relaxation loss realized including the elastic rebound of concrete due to relaxation. Equation can be rewritten as:

$$\Delta f_{pR} = \chi_r \Delta \overline{f}_{pR} K_{idn}$$

According to Tadros, the value χ_r can be given by the following approximation.

$$\chi_r = 1 - \frac{3(\Delta f_{pS} + \Delta f_{pC})}{f_{pi}}$$

Substituting the shrinkage and creep losses calculated for the monitored bridge girders results in values of χ_r close to 0.8. With this value of χ_r,

$$\Delta f_{pR}(t, ti) = \frac{0.8 \log(24(t-ti))}{K'} (\frac{f_{pi}}{f_{py}} - 0.55) f_{pi} K_{idn}$$

With t assumed to be 15,000 days and $K' = 45$ for low-relaxation strands and 10 for other strands, the ultimate relaxation loss is then given by the following equation.

$$\Delta f_{pR} = \frac{1}{K} (\frac{f_{pi}}{f_{py}} - 0.55) f_{pi} K_{idn}$$

Where K is 10 for low-relaxation strands and 2.2 for other strands

2.2.5. NCDOT method

The current NCDOT method for predicting prestress losses is based on the "refined" method specified in the 2004 AASHTO LRFD Bridge Design Specifications. In this method, the predictions of the time-dependent losses are not expressed as functions of time. Rather, they are estimates of the ultimate time-dependent losses only.

The total prestress loss is determined by combining the effects of elastic shortening, concrete shrinkage, creep, and strand relaxation, as follows:

$$\Delta f_{pTL} = \Delta f_{pES} + \Delta f_{pSR} + \Delta f_{pCR} + \Delta f_{R2}$$

Where, $\Delta f_{pES}, \Delta f_{pSR}, \Delta f_{pCR}, \Delta f_{R2} =$ Elastic shortening loss, Shrinkage loss, Creep loss and Relaxation loss respectively

Although some strand relaxation occurs prior to transfer of the pre stressing force, it is commonly accepted that the producer will compensate for this loss by overstressing the strands. Therefore, only the relaxation loss that occurs after transfer is included in the total losses.

a) Loss due to elastic shortening

Elastic shortening loss occurs instantaneously at the time of prestress transfer as a result of the shortening of the girder caused by the application of the prestressing force. This prestress loss is estimated as the product of the stress applied to the concrete at the level of the centroid of the strands and the modular ratio, as follows:

$$\Delta f_{pES} = \frac{E_S}{E_C} f_{cgp}$$

Where, E_S = elastic modulus of the prestressing strand

E_C = elastic modulus of the girder concrete at transfer

f_{cgp} =stress in the concrete at the level of the centroid of the

prestressing strands immediately after transfer due to

prestressing and girder self-weight

$$f_{cgp} = \left(\frac{P_i}{A_g} + \frac{P_i e^2}{I_g} \right) - \frac{M_g e}{I_g} \qquad \text{In which } M_g = \frac{w_g L^2}{8}$$

Where P_i = total prestressing force immediately after transfer

> e = eccentricity of the centroid of the prestressing strands at mid span with respect to the centroid of the girder
>
> A_g = area of the gross cross-section of the girder
>
> I_g = moment of inertia of the gross cross-section of the girder
>
> M_g =moment at mid span due to girder self-weight, assuming simply supported conditions
>
> w_g = uniformly distributed load due to girder self-weight
>
> L= girder length

b) *Loss due to shrinkage*

Shrinkage loss occurs gradually as a result of the shortening of the girder caused by the drying shrinkage of the concrete. It is determined as follows:

$\Delta f_{PSR} = 17 - 0.15 H (ksi)$ Where H= average annual ambient relative humidity (%)

c) *Loss due to creep*

Creep is the time-dependent deformation of the girder concrete caused by sustained stresses due to prestressing, self-weight, and superimposed dead loads. Prestress loss occurs due to the shortening of the girder at the level of the centroid of the strands. In this method, the creep loss is considered to be proportional to the applied stresses. Since the superimposed dead loads are typically applied at a later time than are the prestressing force and self-weight, the stress due to the superimposed dead loads is considered to impact creep less significantly than the other loads.

Where f_{cds} =concrete stress at the level of the centroid of the strands due to superimposed dead loads applied after transfer. $f_{cds} = \dfrac{M_{sd} e}{I_g}$

Where M_{sd} = mid span moment due to superimposed dead loads.

d) Loss due to relaxation

Under the sustained loading of the prestressing force, the strand steel gradually relaxes.

The resulting reduction in prestress is the relaxation loss. This method divides the relaxation loss calculations into two parts, including the loss before transfer and the loss after transfer.

Relaxation loss before transfer

The relaxation loss that occurs between initial stressing and prestress transfer is estimated as follows:

$$\Delta f_{pR1} = \frac{\log(24t)}{40}\left[\frac{f_{pj}}{f_{py}} - 0.55\right]f_{pj}$$

t= time (days) between stressing and transfer.

f_{py}= specified yield strength of the prestressing strands. Taken as 90% of the nominal strength for low relaxation strands

f_{pj}=stress in the strand after jacking. Taken as 75% of the nominal strength

Relaxation loss after transfer

The relaxation loss that occurs after transfer accounts for the interaction with the other components of losses, and is estimated for low relaxation strands as follows:

$$\Delta f_{pR2} = 0.3\big[20 - 0.4\Delta f_{pES} - 0.2(\Delta f_{pSR} + \Delta f_{pCR})\big](ksi)$$

2.2.6. PCI method

The method recommended by the Precast and Prestressed Concrete Institute for estimating prestress losses is similar to the current NCDOT method in that it only estimates the ultimate time-dependent losses rather than time-specific values.

The total prestress loss is the summation of the losses due to elastic shortening, shrinkage, creep, and relaxation, as follows:

$$\Delta f_{pTL} = \Delta f_{pES} + \Delta f_{pSR} + \Delta f_{pCR} + \Delta f_{R2}$$

a) Loss due to elastic shortening

The elastic shortening loss is determined using the same equation used in the NCDOT method, as follows:

$$\Delta f_{pES} = \frac{Ep}{E_{ci}} f_{cgp} \qquad \text{Where} \qquad f_{cgp} = \left[\frac{0.9 p_j}{A_g} + \frac{0.9 p_j e^2}{I_g} \right] - \frac{M_g e}{I_g}$$

P_j = specified jacking force; taken as 75% of the nominal strength multiplied by the total strand area for 270 ksi low-relaxation strands

b) Loss due to shrinkage

This method accounts for the average annual ambient humidity and the volume-to-surface area ratio of the girder. Girders with high volume-to-surface area ratios experience less shrinkage, and vice versa. The shrinkage loss is estimated as follows:

$$\Delta f_{pSR} = (8.2 * 10^{-6}) E_p \left(1 - 0.06 \frac{V}{S} \right) (100 - H)$$

$\frac{V}{S}$ = Volume to surface area ratio of the girder

c) Loss due to creep

Creep loss is proportional to the applied stresses. However, unlike the NCDOT method, this method proportions the stresses due to prestressing and the stresses due to superimposed dead loads equally using the same creep factor of 2.0.

$$\Delta f_{pCR} = 2.0 \frac{E_p}{E_c} (f_{cgp} - f_{cds})$$

d) Loss due to relaxation

For relaxation loss, each loss is treated equally, regardless of when it occurs. This differs from the NCDOT method, in which the elastic shortening loss is given greater influence due to its instant application at transfer. For Grade 270 low-relaxation strand or wire:-

$$\Delta f_{pRE} = (5000 - 0.04(\Delta f_{pSR} + \Delta f_{pCR} + \Delta f_{pES}))$$

$$\Delta f_{pRE} = [K_{re} - J(SH + CR + ES)]C.....(ksi)$$

The values of K_{re} and J depend on the stress level and the material characteristic of the tendon as shown in in table.

Table 2.2 Vales of Kre and J for steel tendon

Types of tendon	K_{re}	J
Grade 270 stress-relieved strand or wire	20,000	0.15
Grade 270 low relaxation strand or wire	5,000	0.04
Grade 145 or 160 stress-relieved bar	6,000	0.05

2.2.7. CEB-FIP method

The following equation was suggested to estimate the long-term prestress losses:

$$\Delta\sigma_{ps} = \frac{\alpha_{ps}\varphi(t,to)f_{cgp} + E_{ps}\varepsilon_{cs} + 0.8\Delta\sigma_{pr}}{1 + \alpha_{ps}\dfrac{A_{ps}}{A_c}(1 + \dfrac{A_c y^2_{ps}}{I_c})(1 + \chi\varphi(t,to))}$$

Where: $\alpha_{ps} = \dfrac{E_{ps}}{E_c}$ = ratio of modulus of elasticity of prestressing steel to that of concrete;

A_{ps} and A_c = areas of pre stressing steel and net concrete section, respectively;

I_c = second moment of area of net concrete section; and

y_{ps} = y-coordinate of prestressing steel measured downwards from centroid of net concrete section.

f_{cgp} = concrete stress at center of gravity of pre stressing steel at transfer;

$\chi = \chi$ is a dimensionless coefficient less than unit = 0.7

$\Delta\sigma_{pr}$ = Reduction in stress is known as intrinsic relaxation

$\phi(t,t_o)$ = The ratio of the creep strain $\varepsilon(t) - \varepsilon(t_o)$ to the instantaneous strain $\varepsilon_c(t_o)$

$$\Delta\sigma_{ps} = \frac{\log(24t)}{40}(\frac{\Delta\sigma_{po}}{fpy} - 0.55)\Delta\sigma_{po}$$

t= time (days) between stressing and transfer.

f_{py}= specified yield strength of the prestressing strands. Taken as 90% of the nominal strength for low relaxation strands

$\Delta\sigma_{p0}$ = Stress in the strand after jacking. Taken as 75% of the nominal strength

2.2.8. Time step method

This method makes use of the AASHTO LRFD time dependent correction factors and the equations for the prediction of losses.

a) Elastic shortening

The Elastic Shortening *ES* is calculated as given below:

$$ES = n * f_{cir}$$

     n = modulus of elasticity of concrete;

     f_{cir} = net compressive stress in concrete at the center of gravity of tendons

           immediately after the pre stress has been applied to the concrete, *ksi*.

The f_{cir} is calculated in two stages, from initial to slab casting and after slab casting. The calculation of f_{cir} for the loading stage after slab casting, utilizes the composite transformed cross section properties of concrete calculated with the use of effective modulus.

b) Loss due to creep

The creep loss is a function of various time dependent factors including the volume to surface ratio, relative humidity and age of concrete at the time of loading. Incremental creep strains are computed daily using the formula:

$$\Delta\varepsilon_{cr}(t) = \left[f_{cir}(t-1)\right]\left[\psi(t,t_i)\right] - \left[\psi(t-t_i,t_i)\right]$$

    $\Delta\varepsilon_{cr}(t)$ = incremental creep strain at time t;

    $\psi(t,t_i)$ = creep coefficient

$$\psi(t,t_i) = 3.5K_cK_f\left(1.58 - \frac{H}{120}\right)t_i^{-0.118}\left(\frac{(t-t_i)^{0.6}}{10+(t-ti)^{0.6}}\right)$$

    K_c = factor for the effect of volume to surface ratio

$$K_c = \left[\frac{\dfrac{t}{26.e^{0.36(V/S)}+t}}{\dfrac{t}{45+t}}\right]\left[\frac{1.8+1.77e^{-0.54(V/S)}}{2.587}\right]$$

K_f = factor for the effect of concrete strength

$$k_f = \frac{1}{0.67 \left(\dfrac{f'c}{9} \right)}$$

H = relative humidity in percent

The creep loss is calculated as given below:

$$CR_{(t)} = CR_{(t-ti)} + \Delta\varepsilon_{cr}(t) * 0.0285$$

c) Loss due to shrinkage

The shrinkage of concrete also depends on the volume to surface ratio and relative humidity, but is independent of the loading and is caused primarily due to shrinkage of cement paste. The shrinkage loss is calculated as given below:

$$SH = E_s * \varepsilon_{sh}$$

E_s = modulus of elasticity of prestressing steel

ε_{sh} = shrinkage strain is calculated

$$\varepsilon_{sh} = -k_s k_h \left(\frac{t}{35+t} \right) 0.51 * 10^{-3}$$

k_s = is size factor given by

$$k_s = \left[\frac{\dfrac{t}{26.e^{0.36(V/S)} + t}}{\dfrac{t}{45+t}} \right] \left[\frac{1064 - 94(V/S)}{923} \right]$$

k_h = humidity factor specified in table 1 of AASHTOO-LRFD manual

d) Loss due to relaxation

Low relaxation strands are most widely used in prestressed girders. The relaxation loss is based on the formula in the AASHTO LRFD equation:

$$RE = \frac{\log(24t)}{40} \left\{ \frac{f_{pi}}{f_{py}} - 0.55 \right\} f_{pi}$$

Where, f_{pi} = initial pre stress at transfer

f_{py} = specified yield strength of prestressing steel

$$\text{Total Loss, } TL = ES + CR + SH + RE.$$

The total loss is calculated by summing up the losses for each day and the prestress, f_{se} and the corresponding prestress force F_{se} is calculated for each stage of loading.

2.3. Prediction of camber and deflection of PSC girder

2.3.1. Introduction

Camber is the common word for the upward deflection of eccentrically prestressed bridge girders. The amount of camber is governed by the combined action of the prestress force which causes the camber and self-weight of the girder to work against the camber. Self-weight and other sustained gravity loads can cause downward deflections to exceed the amount of overall camber. The beams and bridges can deflect downward as a result. Camber and/or deflection are also a function of time dependent concrete creep and prestress loss. Proper estimation of camber or alternatively deflection is essential for an efficient use of longer spans in HPC bridge girders. The camber and deflection of the beam due to prestress and gravity loads were directly computed from the curvature due to concrete strains using moment area method. After slab cast the camber due to the additional creep strain is also included in the final deflection. *(Hema Jayaseelan, Bruce W Russell. Prestress loss and estimation of long term deflection and camber for prestressed concrete member, 2007)*

The camber in a prestressed girder is dependent on many factors: strands properties and configuration, initial prestress losses due to the relaxation of the strands while the girder is still in the casting yard, time dependent effects due to creep and shrinkage, and the sustained loading due to service and self-weight of the structure.

Eccentricity of the prestressing strands in a pre-stressed concrete beam and some small initial prestress losses result in the initial camber of the beam. Elastic shortening and anchorage losses compose the initial pre stress losses.

Long term camber growth is affected by several inter-related time-dependent factors. Creep, shrinkage, and relaxation of the prestressing strands all contribute to a gradual reduction of the effective prestressing force in the strands, which creates prestress losses. Shrinkage, which is a volumetric change, results in a shortening of the beam length. Creep occurs as the concrete deforms under the application of a sustained effective upward load (due to prestressing force eccentricity). Meanwhile, the prestressing strand is itself being subjected to relaxation, which is a loss in prestressing force due to elongation of the stressed strand held at constant length. As the force in the strand decreases from relaxation, shrinkage is also occurring, which further decreases the force in the strand as the beam length shortens. As the force in the strand decreases, the creep inducing upward force component also decreases and the process continues at a decreasing rate as the beam ages. Other factors also affect camber growth, including modulus of elasticity, aggregate type, ambient and curing conditions, and age at release. These factors, along with creep, shrinkage, and relaxation, will now be discussed individually along with the findings of previous researchers. (*Stephen D. Hinkle, Investigation of time dependent deflection in long span, high strength, prestressed concrete bridge beams, 2006*)

2.3.2. Prediction of camber and deflection: N Krishna

1.   Short term camber and deflection in un-cracked PSC girder

Short term or instantaneous camber/deflection of PSC girders are governed by the bending moment distribution along the span and flexural rigidity of the members.
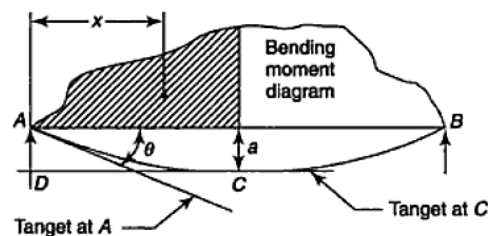
Fig.2.4. Slope and deflection of girder beam

Where θ = slope of elastic curve at *A*

     AD = intercept between the tangent at *C* and vertical at *A*

      a = deflection at the center of symmetrically loaded, simply supported girder

A= area of *B.M.D* between *A* and *C*

x = distance of the centroid of the *B.M.D* between *A* and *C* from the left support

EI = flexural rigidity of the girder

$$\theta = A/EI \quad \text{and} \quad a = Ax/EI$$

i) Camber due to straight tendon

If upward deflections (camber) are considered as negative

P =effective prestressing force, *e* = eccentricity and *L* = length of the member

$$a = \frac{peL^2}{8EI}$$
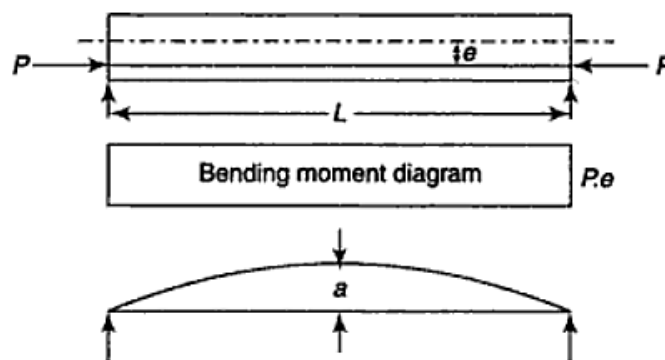
Fig.2.5. Camber of girder beam under eccentric straight tendon

ii) Camber due to trapezoidal tendon

$$a = \frac{pe}{6EI}[2l_1^2 + 6l_1l_2 + 3l_1^2]$$
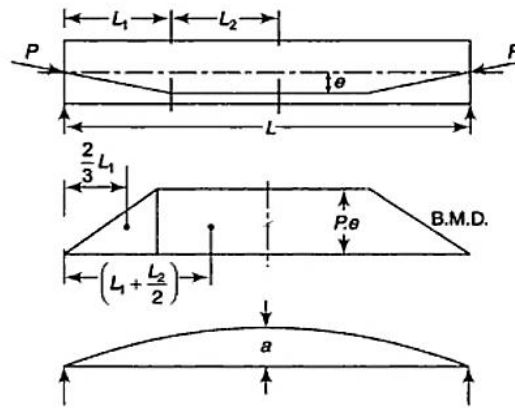
Fig.2.6. Camber of girder beam under eccentric trapezoidal tendon

iii)   *Camber due to parabolic tendons (central anchor)*

$$a = \frac{5\,peL^2}{48EI}$$
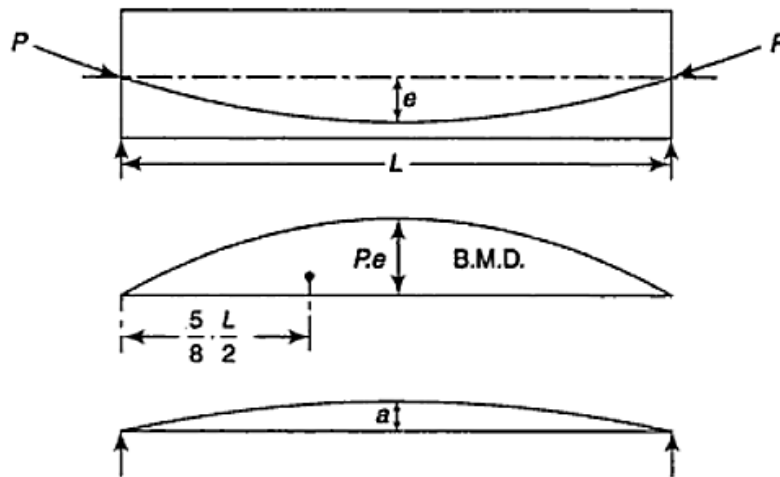
Fig.2.7. Camber of girder beam under eccentric parabolic tendon (central anchor)

iv) *Camber due to parabolic tendons (eccentric anchor)*

$$a = \frac{pL^2}{48EI}[-5e_1 + e_2]$$
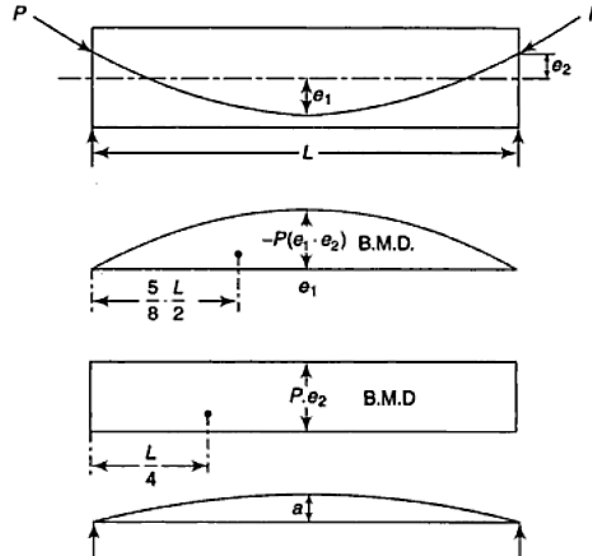
Fig.2.8. camber of girder beam under eccentric parabolic tendon (eccentric anchor)

v)   Deflection due to self-weight and imposed loads

If g (self-weight of girder beam/m) and q (imposed load/m) down ward deflection is given by:

$$a = \frac{5[g+q)L^4}{384EI}$$

2. Prediction of long term deflection un-cracked PSC girder

The deformation of PSC member change with time as a result of creep, shrinkage and. The PSC member develops deformations under the influence of two usually opposing effects, which are the prestress and the transverse loads. The net curvature ϕ_t at a section at any given stage is obtained by:

$$\phi_t = \phi_{mt} + \phi_{pt}$$

ϕ_{mt} = change of curvature caused by transverse load

ϕ_{pt} = change of curvature caused by prestress

Under the section of sustained transverse load, the compressive stress distribution in the concrete changes with time. The creep strain due to transverse load is directly computed

as a function of the creep coefficient. So that the change of curvature can be estimated by:

$$\phi_{mt} = (1 + \phi) \phi_i$$

Where ϕ = creep coefficient and ϕ_i = initial

According to Neville and ACI committee report the creep curvature due to prestress is obtained on the simplified approach as follows:

P_i = initial pre stress and P_t = pre stress after time t.

Loss of prestressing force due to relaxation, shrinkage and creep, $L_p = P_i \text{-} P_t$

For e = eccentricity of prestressing and EI = flexural rigidity, the curvature due to prestress after time t can be expressed as:

$$\phi_{pt} = -\frac{p_i e}{EI}[1 - \frac{L_p}{P_i} + (1 - \frac{L_p}{2P_i})\phi]$$

If a_{i1} (initial deflection due to transverse loads) and a_{ip} (initial deflection due to prestress), then the total long term deflection after time t is given by:

$$a_f = a_{i1}(1 + \phi) - a_{ip}[(1 - \frac{L_p}{P_i}) + (1 - \frac{L_p}{2P_i})\phi]$$

A simplified but approximate expression is suggested by Lin for computing long term deflection. According to this method the final long term deflection is:

$$a_f = [a_{i1} - a_{ip} * \frac{P_t}{P_i}](1 + \phi)$$

2.3.3. NCDOT method

The NCDOT method is a multiplier method that predicts camber at the time of prestress transfer and at the time of bridge erection

a)   *Camber at transfer*

The two components of net camber at the time of transfer are the *upward deflection* due to prestressing and the *downward deflection* due to self-weight. The net camber is determined as follows: $\Delta_i = \Delta_{ps,i} - \Delta_{sw,i}$

Where Δ_i = net camber at transfer

$\Delta_{ps,i}$ = upward deflection due to prestressing

$$\Delta_{ps,i} = \frac{P_i}{E_{ci}I_g}\left(\frac{e_m L^2}{8} - (e_m - e_e)\frac{(L/2 - x_h)^2}{6}\right)$$

$\Delta_{sw,i}$ = downward deflection due to girder self-weight

$$= \frac{5w_g L^4}{384 E_{ci}I_g} + \Delta diaphram$$

P_i = prestressing force immediately after transfer

e_m = eccentricity of the centroid of the strands at mid span with respect to the centroid of the gross section

e_e = eccentricity of the centroid of the strands at the end of the girder with respect to the centroid of the gross section. De bonding is neglected.

L = girder length

E_{ci} = elastic modulus of the concrete at transfer

I_g = moment of inertia of the gross section

W_g = linearly distributed self-weight load

X_h = distance from harp point to center of span deflection due to internal diaphragms in hollow girders;

$\Delta_{diaphram}$ = diaphragms are treated as point loads; deflection depends on number and location; zero for solid girders.

b)   *Camber at time of bridge erection*

To estimate the net camber at the time of bridge erection, the components of initial deflection at transfer are adjusted by multipliers. The downward deflection due to superimposed loads applied at bridge erection is also included if superimposed loads are present:

$$\Delta = 2.26\Delta_{ps,i} - 2.31\Delta_{sw,i} - \Delta_{sd}$$

Where:

Δ = net camber (upward + down ward deflection)

Δ_{sd} = deflection due to superimposed dead loads applied at bridge erection

$$= \frac{5w_{sd}L^4}{384E_cI_g}$$

w_{sd} = weight of superimposed loads applied at bridge erection

E_c = elastic modulus of the concrete at bridge erection

2.3.4. PCI method

The PCI method also uses multipliers to predict camber at prestress transfer, at bridge erection, and at an arbitrary "final" time in the distant future, which represents the ultimate deflection.

a) Camber at transfer

The calculation of the camber at prestress transfer is identical to the NCDOT method

b) Camber at time of bridge erection

In estimating the camber at the time of bridge erection, the PCI method is similar to the NCDOT method except that the multipliers are reduced:

$$\Delta = 1.8\Delta_{ps,i} - 1.85\Delta_{sw,i} - \Delta_{sd}$$

Where $\Delta p_{s,i}$, $\Delta p_{sw,i}$ and Δ_{sd} are calculated according to NCDOT method

c) Camber at final time

The net camber at an arbitrary "final" time in the distant future is estimated using additional multipliers for the initial deflections. The deflection due to superimposed loads applied at bridge erection, if such loads are present, is also adjusted by a multiplier.

$$\Delta = 2.45\Delta_{ps,i} - 2.7\Delta_{sw,i} - 3\Delta_{sd}$$

If the superimposed load applied at bridge erection is a composite topping, then its contribution to deflection is multiplied by 2.30 instead of 3.00 in the above equation.

2.4. NCHRP 496 specification

2.4.1. Recommended specification

The detailed losses procedure proposed by the National Cooperative Highway Research Program (NCHRP) Report 496, by Tadros, et al(2003) make use of the aging coefficient approach for the computation of losses between the transfer and casting of the decks. The method covers the composite action between the precast concrete girders and cast-in-place deck slab. The prestress losses are computed in four stages:

a) Instantaneous prestress loss due to elastic shortening at transfer, Δf_{pES}

b) Long-term prestress losses due to shrinkage of concrete, $(\Delta f_{pSR})_{id}$, and creep of concrete, $(\Delta f_{pCR})_{id}$ and relaxation of prestressing strands, $(\Delta f_{pR2})_{id}$, between the time of transfer and just before deck placement.

c) Instantaneous prestress gain due to the placement of deck weight Δf_{pED}

d) Long-term prestress losses between the time of deck placement and the final service life of the structure, due to shrinkage of the girder, $(\Delta f_{pED})_{df}$ creep of the girder, $(\Delta f_{pCD1} + \Delta f_{pCD2})_{df}$, relaxation of prestressing strands, $(\Delta f_{pR3}+)_{df}$, and shrinkage of deck concrete, $(\Delta f_{pSS})_{df}$

The total prestress loss in the pre-tensioned bridge girder is given by:

$$\Delta f_{pT} = \Delta f_{pES} + (\Delta f_{pSR} + \Delta f_{pCR} + \Delta f_{pR2})_{id} - \Delta f_{pED} + (\Delta f_{pSD} + \Delta f_{pCD1} + \Delta f_{pCD2} + \Delta f_{pR3} - \Delta f_{pSS})_{df} \, (ksi)$$

a) *Loss due to elastic shortening*

$$\Delta f_{pES} = n_i f_{cgp} \text{ Where } n_i = \frac{E_p}{E_{ci}}$$

f_{cgp} = concrete stress at the center of gravity of the prestressing force;

$$f_{cgp} = P_i \left(\frac{1}{A_{ti}} + \frac{e^2_{pti}}{I_{ti}} \right) - \frac{M_g e_{pti}}{I_{ti}} ksi$$

     P_i = initial prestressing force just before release, kips;

     A_{ti} = initial transformed area of cross section at release, in

     I_{ti} = initial transformed moment of inertia, in4;

     e_{pti} = initial eccentricity of strands with respect to the transformed cross section, in;

     M_g = maximum moment due to self-weight of the girder, kip-in

b) *Loss due to shrinkage*

$$\Delta f_{pSR} = \varepsilon_{bid} E_p K_{id}$$

Where, ε_{bid} = concrete shrinkage strain of the girder between transfer and deck placement;

     K_{id} = transformed section age-adjusted effective modulus of elasticity factor, for

     adjustment between time of transfer and deck placement;

$$= \frac{1}{1 + n_i \rho_n \alpha_n (1 + \chi \psi_{bif})}$$

ψ_{bif} = girder creep coefficient between the transfer and final;

χ = aging coefficient that accounts for the variability of concrete stress with time, and may be considered constant for all concrete members at age 1 to 3 days. (0.7 averages);

ρ_n = tensile reinforcement ratio for the initial section; $= \dfrac{A_{ps}}{A_n}$

A_{ps} = area of the prestressing strands, in^2;

A_n = area of net concrete section, in^2;

α_n = factor for initial net section properties;

$$\alpha_n = \left(1 + \frac{A_n e^2{}_{pn}}{I_n}\right)$$

e_{pn} = eccentricity of the prestressing strands with respect to net concrete section, in;

I_n = moment of inertia of the net concrete section, in^4.

c) *Loss due to creep*

$$\Delta f_{pCR} = n_i f_{cgp} \psi_{bid} K_{id}$$

Where,

ψ_{bif} = girder creep coefficient between the transfer and deck placement.

d) *Loss due to relaxation of prestressing strands*

$$\Delta f_{pR2} = \phi_i L_i K_{id} ,..(ksi)$$

Where, ϕ_i= reduction factor that reflects he steady decrease in strand prestressing due to

creep and shrinkage of concrete;

$$\phi_i = 1 - \frac{3(\Delta f_{pSR} + \Delta f_{pCR})}{f_{po}} ,..(ksi)$$

$$L_i = \left[\frac{\log\left(\dfrac{24 t_d + 1}{24 t_i + 1}\right)}{45} \right] \left[\frac{f_{po}}{f_{py}} - 0.55 \right] f_{po} ,..(ksi)$$

L_i= intrinsic relaxation loss between transfer and placement of deck slab;

f_{po} = stress in the prestressing strands just after release, ksi;

t_d = age of the concrete after the placement of deck, days;

t = age of the concrete at the time of transfer, days.

Since the relaxation loss of the low-relaxation strands is very small ranging from 1.5 ksi to 4.0 ksi, a constant value of 2.4ksi is assumed.

2.4.2. AASHTO LRFD 2010 Specification

The method specified in the AASHTO LRFD Bridge Design Specifications can be used to estimate prestress losses at any time. In addition, the predictions of the time dependent losses are calculated in two parts: the losses occurring before deck placement and those occurring after deck placement. The calculations for this method are more detailed than are those for the NCDOT and PCI methods. One major reason is that the creep loss and shrinkage loss calculations also require the calculation of creep coefficients and shrinkage strains. This method also includes provisions to account for the effects of composite deck systems.

Creep Coefficient

The general form of the equation for the creep coefficient at a time is as follows:

$$\psi(t_2, t_1) = 1.9 k_s k_{hc} k_f k_{td} t_1^{-0.118}$$

Where:-k_s=factor to account for the effect of the volume to surface ratio

$$= 1.45 - 0.13 \frac{V}{S} \geq 0$$

$k_{hc} = 1.56 - 0.008H$,….humidity factor for creep

$$k_f = \frac{5}{1 + f'_{ct}} ,….. \text{factor for effect of concrete strength}$$

$$k_{td} = \frac{t_2 - t_1}{61 - 4f'_{ct} + (t_2 - t_1)} ,…\text{time development factor}$$

t_1= age of concrete at time of loading for creep calculation or at time of

prestress transfer for shrinkage calculation (days)

t_2= age of concrete at time of consideration of creep or shrinkage effect (days)

f'_{ct}= specified compressive strength of concrete at time of prestressing

The creep coefficient for the period between times   and   due to loading applied at time is determined as follows:

$$\psi(t_3,t_2) = \psi(t_3,t_1) - \psi(t_2,t_1)$$

Where $\psi(t_3,t_1)$ = creep coefficient at time t_3 due to loading applied at time t_1

$\psi(t_2,t_1)$ = creep coefficient at time t_2 due to loading applied at time t_1

Shrinkage Strain

The concrete shrinkage strain is determined by applying various factors to a base shrinkage strain of 0.48×10^{-3}. The factors account for the effects of concrete strength, ambient humidity, volume to surface area ratio, and time. The general form of the equation for shrinkage strain is as follows:

$$\varepsilon_{sh} = k_s k_{hs} k_f k_{td} \, 0.48 * 10^{-3}$$

Where:- k_{hs} = 2-0.014H ,….humidity factor for shrinkage

$k_{td} = \dfrac{t}{61 - 4f'_{ct} + t}$,…time development factor

t= time between prestress transfer & time under consideration (days)

The total pre stress loss is the summation of all of the losses:

$$\Delta f_{pTL} = \Delta f_{pES} + (\Delta f_{pSR} + \Delta f_{pCR} + \Delta f_{R1}+)_{id} + (\Delta f_{pSD} + \Delta f_{pCD} + \Delta f_{pR2} - \Delta f_{pSS})_{df}$$

Where: - $(\Delta f_{pSR} + \Delta f_{pCR} + \Delta f_{R1})_{id}$ = summation of time dependent losses between time of

prestress transfer and time of deck placement

$(\Delta f_{pSD} + \Delta f_{pCD} + \Delta f_{pR2} - \Delta f_{pSS})_{id}$ = time dependent losses occurring after deck placement

a) Elastic Shortening

The elastic shortening loss is determined using the same procedure as described by the NCDOT method

b) Loss due to shrinkage

The time-dependent shrinkage loss is calculated in two steps, including the loss occurring prior to deck placement and the loss occurring after deck placement. The times can be adjusted to predict the loss at any time.

Prior to deck placement

The shrinkage loss that occurs prior to deck placement is determined by first calculating the concrete shrinkage strain at the time of deck placement. This strain is then converted into pre stress loss using the elastic modulus of the strands. Finally, a time development factor is used to account for the time-dependent interaction between the concrete and the bonded steel. The shrinkage loss is determined as follows:

$$\Delta f_{pSR} = \varepsilon_{bid} E_p K_{id}$$

Where: ε_{bid} =concrete shrinkage strain at time of deck placement

K_{id}= transformed section coefficient at accounts for time dependent interaction

between concrete and bonded steel in the section being considered for the

time period between transfer and deck placement

$$K_{id} = \frac{1}{1 + \dfrac{E_p A_{ps}}{E_{ci} A_g}\left(1 + \dfrac{A_g e^2}{I_g}\right)\left(1 + 0.7\psi(t_f, t_1)\right)}$$

A_{ps} = total area of prestressing strand

$\psi(t_f, t_1)$ = ultimate creep coefficient due to loading applied at transfer

After deck placement

The shrinkage loss after deck placement is determined in a manner similar to the shrinkage loss before deck placement, as follows:

$$\Delta f_{pSD} = \varepsilon_{bdf} E_p K_{df}$$

Where: ε_{bdf} = shrinkage strain for the period between deck placement and the final time

K_{df} = time development factor for the period between deck placement and the final time

$$= \frac{1}{1 + \dfrac{E_p A_{ps}}{E_{ci} A_g} \left(1 + \dfrac{A_c e^2_{pc}}{I_c}\right)\left(1 + 0.7\psi(t_f, t_1)\right)}$$

A_c = area of section calculated using the gross composite concrete section properties of the girder and the deck and the deck to girder modular ratio

A_c = moment of inertia of the section calculated using the gross composite concrete section properties of the girder and the deck and the deck to girder modular ratio at service

e_{pc} = eccentricity of the prestressing force with respect to the centroid of the composite section

c) *Loss due to creep*

The time-dependent creep loss prediction is also separated into two   parts, including the loss occurring prior to deck placement and the loss occurring after deck placement.

Prior to deck placement

The creep loss that occurs prior to deck placement is determined as follows:

$$\Delta f_{pCR} = \frac{E_p}{E_{ci}} f_{cgp} \psi(t_d, t_i) K_{id}$$

$\psi(t_d, t_i)$ =creep coefficient at time of deck placement due to loading applied at transfer

t_d= age of concrete at time of deck placement (days)

After deck placement

The pre stress loss (if positive) or gain (if negative) due to creep that occurs after deck placement is determined as follows:

$$\Delta f_{pCD} = \frac{E_p}{E_{ci}} f_{cgp} (\psi(t_f, t_i) - \psi(t_d, t_i)) K_{df} + \frac{E_p}{E_c} \Delta f_{cD} \psi(t_f, t_d) K_{df}$$

Δf_{CD} = change in concrete stress at the centroid of the strands due to time- dependent losses between transfer and deck placement, combined with deck weight and super imposed loads. Negative if compressive concrete stress is reduced

d) Loss due to relaxation

Prior to deck placement

The relaxation loss that occurs prior to deck placement is estimated as follows:

$$\Delta f_{pR1} = \frac{f_{pi}}{30} \left(\frac{f_{pi}}{f_{py}} - 0.55 \right)$$

f_{pi} = stress in prestressing strands immediately after transfer

$$= f_{pj} - \Delta f_{pES}$$

After deck placement

The relaxation loss occurring after deck placement is considered to be equal to the relaxation loss before deck placement:

$$\Delta f_{pR2} = \Delta f_{pR1}$$

2.4.3. Euro code 2 Specification

a) Prestressing force

At a given time t and distance x (or arc length) from the active end of the tendon the mean prestress force $P_{m,t(x)}$ is equal to the maximum force P_{max} imposed at the active end, minus the immediate losses and the time dependent losses. Absolute values are considered for all the losses.

The value of the initial prestress force $P_{mo(x)}$ (at time $t = t_o$) applied to the concrete immediately after tensioning and anchoring (post-tensioning) or after transfer of prestressing (pre-tensioning) is obtained by subtracting from the force at tensioning P_{max} the immediate losses $\Delta P_{i(x)}$ which should not exceed the following value:

$$P_{mo(x)} = A_p \cdot \sigma_{pmo(x)}$$

Where: $\sigma_{pmo(x)}$ is the stress in the tendon immediately after tensioning or transfer

$$\sigma_{pmo(x)} = \min \{ k_7 \cdot f_{pk} ; k_8 f_{p0,1k} \}$$

The values for k_7 is 0.75 and for k_8 is 0.85

When determining the immediate losses $\Delta P_{i(x)}$ the following immediate influences should be considered for pre-tensioning and post-tensioning.

- o   losses due to elastic deformation of concrete ΔP_{el}
- o   losses due to short term relaxation ΔP_r
- o   losses due to friction $\Delta P_\mu(x)$
- o   losses due to anchorage slip ΔP_{sl}

The mean value of the prestress force $P_{m,t(x)}$ at the time $t > t_0$ should be determined with respect to the prestressing method. In addition to the immediate losses the time dependent losses of prestress $\Delta P_{c+s+r}(x)$ as a result of creep and shrinkage of the concrete and the long term relaxation of the prestressing steel should be considered and

$$P_{m,t(x)} = P_{mo(x)} - \Delta P_{c+s+r}(x)$$

b) *Immediate losses of prestress for pre-tensioning*

- During the stressing process: loss due to friction at the bends (in the case of curved wires of strands) and losses due to wedge draw-in of the anchorage devices.

- Before the transfer of prestress to concrete: loss due to relaxation of the pre-tensioning tendons during the period which elapses between the tensioning of the tendons and prestressing of the concrete.

- At the transfer of prestress to concrete: loss due to elastic deformation of concrete as the result of the action of pre-tensioned tendons when they are released from the anchorages.

c) *Immediate losses of prestress for post-tensioning*

Losses due to the instantaneous deformation of concrete ΔP_{el}

$$\Delta P_{el} = A_p . E_p . \Sigma \left[\frac{j.\Delta\sigma_c(t)}{E_{cm}(t)} \right]$$

$\Delta\sigma_c(t)$: is the variation of stress at the center of gravity of the tendons applied at time t

j: is a coefficient equal to *(n-1)/2n* where *n* is the number of identical tendons successively prestressed. As an approximation this may be taken as **½**

Losses due to friction $\Delta P_{\mu}(x)$

The losses due to friction $\Delta P\mu(x)$ in post-tensioned tendons may be estimated from:

$$\Delta P_{\mu}(x) = P_{max}\left(1 - e^{-\mu(\theta + kx)}\right)$$

θ= is the sum of the angular displacements over a distance x (irrespective of sign)

μ= is the coefficient of friction between the tendon and its duct

k= is an unintentional angular displacement for internal tendons (per unit length)

x= is the distance along the tendon from the point where the prestressing force is equal

to P_{max} (the force at the active end during tensioning)

The value μ given in table 5.1 of Euro code 2 and depends on the surface characteristics of the tendons and the duct, on the presence of rust, on the elongation of the tendon and on the tendon profile.

The value k for unintentional angular displacement depends on the quality of workmanship, on the distance between tendon supports, on the type of duct or sheath employed, and on the degree of vibration used in placing the concrete.

Losses at anchorage

Account should be taken of the losses due to wedge draw-in of the anchorage devices, during the operation of anchoring after tensioning, and due to the deformation of the anchorage itself.

d) Time dependent losses of prestress for pre- and post-tensioning

The time dependent losses may be calculated by considering the following two reductions of stress:

- Due to the reduction of strain, caused by the deformation of concrete due to creep and shrinkage, under the permanent loads:
- The reduction of stress in the steel due to the relaxation under tension.

A simplified method to evaluate time dependent losses at location x under the permanent loads is given by:

$$\Delta P_{c+s+r} = A_p \Delta\sigma_{p,c+s+r} = A_p \frac{\varepsilon_{cs} E_p + 0.8\Delta\sigma_{pr} + \dfrac{E_p}{E_{cm}}\varphi(t,t_o).\sigma_{c,QP}}{1 + \dfrac{E_p}{E_{cm}}\dfrac{A_p}{A_c}\left(1 + \dfrac{A_c}{I_c}Z^2_{cp}\right)\left(1 + 0.8\varphi(t,t_o)\right)}$$

$\Delta\sigma_{p,c+s+r}$ = is the absolute value of the variation of stress in the tendons due to creep, shrinkage and relaxation at location x, at time t

ε_{cs} = is the estimated shrinkage strain in absolute value according to 3.1.4(6)

E_p = is the modulus of elasticity for the prestressing steel according to 3.3.3 (9)

E_{cm}= is the modulus of elasticity for the concrete according to table 3.1

$\Delta\sigma_{pr}$ = is the absolute value of the variation of stress in the tendons at location x, at time t, due to the relaxation of the prestressing steel. It is determined for a stress of

$$\sigma_p = \sigma_p(G+P_{m0}+ \psi_2 Q)$$

$\sigma_p = \sigma_p(G+P_{m0}+ \psi_2 Q)$ is the initial stress in the tendons due to initial prestress and quasi-permanent actions.

$\phi(t,t_0)$ = is the creep coefficient at a time t and load application at time t_0

$\sigma_{c,QP}$ = is the stress in the concrete adjacent to the tendons, due to self-weight and initial prestress and other quasi-permanent actions where relevant. The value of $\sigma_{c,QP}$ may be the effect of part of self-weight and initial prestress or the effect of a full quasi-permanent combination of action $\sigma_c(G+P_{m0}+ \psi_2 Q)$ depending on the stage of construction considered.

A_p = is the area of all the prestressing tendons at the level being considered.

A_c = is the area of the concrete section.

I_c = is the second moment of area of the concrete section.

Z_{cp}=is the distance between the center of gravity of the concrete section and the tendons

2.5.   Traffic analysis to account for Fatigue load

2.5.1. Introduction

The deterioration of bridge is caused by traffic results from the magnitude of the individual wheel loads, the number of times these loads are applied and Environmental factors. Hence, to design a highway bridge, it is necessary to consider not only the traffic volume or the total number of vehicles that will use the road but also to predict the number of repetitions of each axle load group (or wheel load group) during the design period. To convert the traffic volumes into cumulative equivalent standard axle loads (ESAL or CESAL which is one design parameter in bridge design) equivalency factors are used.

In this section, method of determining the traffic volume and CESAL with reference to Ethiopian Roads Authority (ERA) Bridge Design Manual will be discussed. There are three different procedures for considering traffic effects.

1) Fixed traffic procedure

In fixed traffic procedure, the design is made for a single wheel load only and the number of load repetition is not considered. If the bridge is subjected to multiple wheels, they must be converted to an equivalent single wheel load (ESWL), so that the design method based on single wheel can be applied. This method has been used most frequently for heavy wheel loads but light traffic volume.

2) Variable Traffic and Vehicle

In this procedure, both traffic and vehicle are considered variable, so there is no need to assign an equivalent factor for each axle load. The various axle loads can be divided into a number of groups and the stresses, strains and deflections under each load group can be determined separately and used for design purposes. This procedure is most suited to mechanistic methods of design, wherein the responses of pavement under different loads can be evaluated by using a computer.

3) Fixed vehicle Procedure

In this procedure, the bridge is governed by the number of repetitions of a standard vehicle or axle load (usually 80kN single axle load). Axle loads which are not equal to 80kN or consist of tandem or tridem axles must be converted to an 80kN single-axle load by an equivalent axle load factor (EALF). EALF is defined as the damage per pass to a bridge by the axle in question relative to the damage per pass of a standard axle load, (80KN). The number of repetitions under each single or multiple axle loads must be multiplied by its EALF to obtain the equivalent effect based on an 80kN single axle load.

A summation of the equivalent effects of all axle loads during the design period results in an equivalent single axle load (ESAL). Due to the great varieties of axle loads and traffic volumes and their intractable effects on bridge performance, most of the design methods in use today are based on the fixed vehicle procedure.

2.5.2. Design Period

The length or duration of time during which the bridge is expected to function satisfactorily without the need for major intervention (rehabilitation such as overlays or reconstruction) or the duration in time until the bridge structure reaches its terminal condition (failure condition). Selecting appropriate design period depends on:-

- o Functional importance of the bridge
- o Traffic volume
- o Location and terrain of the bridge
- o Financial constraints
- o Difficulty in forecasting traffic

Longer design period is for important roads, high traffic volume, roads in difficult location and terrain where regular maintenance is costly and difficult due to access problems or lack of construction material. Short Design Period if there is problem in traffic forecasting, financial constraints, etc.

2.5.3. Determination of traffic volume

i) Vehicle classification

Small axle loads from private cars and other light vehicles do not cause significant bridge damage. Damage is caused by heavier vehicles (commercial vehicles). Hence, it is important to distinguish the proportion of vehicles which cause bridge damage (commercial vehicles) from total traffic

Table 2.3 ERA vehicle classification system

Vehicle Code	Type of Vehicle	Description
1	Small car	Passenger cars, minibuses (up to 24-passenger seats), taxis, Pick-ups, and Land Cruisers, Land Rovers, etc.
2	Bus	Medium and large size buses above 24 passenger seats
3	Medium Truck	Small and medium sized trucks including tankers up to 7 tons load
4	Heavy Truck	Trucks above 7 tons load
5	Articulated Truck	Trucks with trailer or semi-trailer and Tanker Trailers

ii) Traffic count

Traffic count is necessary

- o   To assess the traffic-carrying capacity of different types of bridge
- o   Examine the distribution of traffic between the available traffic lanes
- o   In the preparation of maintenance schedules for in-service bridge
- o   In the forecasting of expected traffic on a proposed new bridge from traffic studies on the surrounding road system

Traffic volume data determined from

- Historical traffic data available in relevant authorities (ERA conducts regular 3 times a year (Feb., Jul., Nov.) traffic counts on its major road network) and/or
- By conducting classified traffic counts:

> On the bridge : if the bridge is an existing and the project is Upgrading, Rehabilitation, Maintenance, etc.
>
> On other parallel routes and/or adjacent bridge : for new bridge

iii) ADT (Average Daily Traffic)

ADT is determined from the traffic count data as follows: Adjust the 16hrs traffic count data into 24hrdata by multiplying with the average night adjustment factor

Night adjustment factor = (24hr traffic)/ *(16hr traffic):- obtained from the two days 24hr count data.*

(ADT) o= the current ADT= Average of the 7 days 24hr traffic volume data

iv) (AADT)o Annual Average Daily Traffic

   (AADT)$_O$ = total annual traffic in both directions divided by 365

In order to capture the average annual traffic flow trend, adjustment must be made for seasonal traffic variation. Hence traffic count as above must be made at different representative seasons (ERA conducts traffic counts on February, July and November). Make adjustment to (ADT) o based on the season at which the current traffic count belongs to and based on seasonal adjustment factors for the bridge (or similar bridge) derived from historic traffic data (ERA or other regional/national sources)

   (AADT)o = (ADT)o adjusted for seasonal variation

v) Axle load survey

Axle load survey is carried out together with the traffic count and Portable vehicle (wheel) weighing devices or weigh in motion (WIM) devices can be used for surveying. Each axle of the vehicle is weighed and EALF computed for each axle as follows

$$EALF = \left(\frac{L_x}{80}\right)^{4.5}.$$

According to ERA design manual each axle of a tandem axle or tridem axle assembly is considered as one repetition and EALF calculated for each axle i.e. a tandem axle constitutes 2 load repetitions and a tridem axle constitutes 3 load repetitions.

vi) Truck factor

Truck factor can be computed for each vehicle by summing up the number of ESAL per vehicle. Average truck factor can be computed for each vehicle category (for example for Buses, Light Trucks, Medium Trucks, etc.), by summing up the ESAL of all the vehicles in each category and dividing by the number of vehicles (of that category) weighed.

$$TF_i = \frac{\sum_{j=1}^{n} ESAL_j}{n}$$

Where TF_i = Truck factor for the ith vehicle category

n = number of ith vehicles category weighed during the axle load survey

$ESAL_j$ = number of equivalent standard axle loads for the jth vehicle

vii) Design traffic loading

The data and parameters obtained from the studies discussed in the preceding sections can now be used to estimate the design cumulative design traffic volume and loading.

i)　　Adjustment for lane and directional Distribution of traffic.

Lane Distribution Factor (P): accounts for the proportion of commercial vehicles in the design lane. For two lane highways, the lane in each direction is the design lane, so the lane distribution factor is 100%. For multilane highways, the design lane is the heavily loaded lane (outside lane).

Table 2.4.Lane distribution factors (ERA/AASHTO)

Number of Lanes in each direction	Percent Traffic (ESAL) in design lane
1	100
2	80 – 100
3	60 – 80
4	50 – 7

Directional Distribution Factor (D): factor that accounts for any directional variation in total traffic volume or loading pattern. It is usually 0.5 (50%). However, could be adjusted based on actual condition (if there is directional tendency to commercial vehicle distribution (volume or loading); for example if the heavy vehicles in one direction are loaded and come back empty in the other direction).

ii)　　Calculating $(AADT)_1$

AADT1, Annual Average Daily Traffic (both directions) at year of bridge opening (year at which construction works are completed and the bridge is made open for traffic). If time between traffic count year (design time) and estimated year of bridge opening = x, then

$$AADT_1 = AADT_0 \, (1+r)^{\,x}$$

iii)　　Cumulative Traffic Volume (T),

Can be computed for all traffic (T) or for each vehicle   class (Ti)

$$Ti = 365 \, (P) \, (D) \, AADT_{1i} \, [(1+r_i)^{\,N} - 1] / (r_i)$$

Where, Ti = cumulative volume of traffic for the ith vehicle class in the design lane over

the design period (adjusted for lane distribution and direction).

r_i= annual growth rate for the ith commercial vehicle class

P = Lane distribution factor; D = Directional distribution factor

N = Design Period in years

iv) Design traffic (Cumulative Equivalent Standard Axle Load - CESAL)

Computed by multiplying the total traffic volume for each vehicle category (Ti) by its corresponding truck factor (TF_i)

$$Design\ traffic\ load = CESAL = \sum(Ti * TFi)$$

Table 2.5: ESA for different heavy vehicle configurations

Vehicle Type	Average ESAs per Vehicle	Typical Range of Average ESAs per Vehicle
2-axle truck	0.70	0.30 – 1.10
2-axle bus	0.73	0.41 – 1.52
3-axle truck	1.70	0.80 – 2.60
4-axle truck	1.80	0.80 – 3.00
5-axle truck	2.20	1.00 – 3.00
Others	0	0

CHAPTER THREE – RESEARCH METHODOLOGY

3.1.   Introduction

The methodology to carry out this research work is done by focusing on review of different literature reviews, journals from the Internet in addition to the locally available books and journals that are related to the research work.

The prediction is done by MATLAB and MATHCAD PRIME. These two computer languages are mainly applicable to the field of engineering to simplify manual computations and to make ease of work.

3.2.   Study Area

Since the thesis is a case study, a prestressed AWASH bridge constructed on 2014 G.C is under consideration for the prediction of long term or time dependent serviceability related behaviors (pre stress losses and net deflection) up to the end of 2030 G.C.

3.3.   Study design

This research is analytical study that talks about how service ability, performance and capacity of a PSC bridge is affected under fatigue load with respect to some parameters. In this study prediction of two parameters (loss and deflection) were studied.

3.4.   Population

Population studied in this research is PSC box -girder Bridges with respect to their time dependent service ability behaviors (losses and deflection)

3.5.   Sample size and Sampling procedures

The research or program developed is concerned with PSC box -girder bridges available and a single sample (Alternative Awash Bridge) is selected for case study.

3.6. Study variables

There are dependent and independent variables that are closely related with long term (time dependent) serviceability behavior of the bridge. The variable includes that:

- ❑ Pre stress loss *(dependent variable)*
- ❑ Deflection*(dependent variable)*
- ❑ Magnitude of pre stressing force*(independent variable)*
- ❑ No & size of steel tendons
- ❑ Eccentricity(e) of tendon profile from the centroid*(ind.t variable)*
- ❑ Cross sectional dimension of girder*(ind.t variable)*
- ❑ Magnitude of gravitational (dead and live) load *(ind.t variable)*
- ❑ Strength of material (concrete and steel) *(indep.t variable)*
- ❑ Time (t) at which serviceability is to be predicted*(indep.t variable)*

3.7. Data collection process

I)Structural analysis and design review

To carry out this research data (variables) from analysis and design of box girder Bridge under consideration is collected from ERA. And specified specification i.e. AASHTO, ERA design manual, title related journals and materials are also helpful.

II) Collection of traffic data: ADT and AADT along the route is under consideration

3.8. Data processing and analysis

After data is collected among different sample according to the previous section, then the collected data is selected, processed, and analyzed.

Based upon collected data, the computer program written pass throughout the following procedures/ steps.

Step 1: Input parameters

The following parameters are obtained from ERA for Awash PSC Bridge:

- ➢ Design output
- ➢ Traffic data or *AADT* of the route

Step2: data processing and computing

> ➢ The program is developed based upon input data to obtain the desired output

Step 3: Program output or result

> ➢ Total pre stress loss at time (t)
> ➢ Net deflection of bridge at time (t)

The overall procedures and algorithm through which this research carried out is summarized in a flow chart shown in figure 3.1. The flow chart starts from primary input data obtained from design output and it shows computations of long term serviceability behavior of PSC bridge specifically prestress losses and long term deflection. The flow chart ends with result and discussion about these serviceability behaviors in relation with time and fatigue load.

3.9. Ethical considerations

To obtain data from design officials, a consent letter from JIT was written and issue related organization is informed. The data collected was used only for research purposes in order to ensure the confidentiality of the data. The data was collected honestly and based on the willingness of informants or organizations to give information.

1. Enter design output (length, cross-sectional dimensions, number and size of steel tendons
2. Enter material properties
3. Enter parameters for instantaneous losses
4. Enter time at which prediction is to be taken and maximum time of prediction
5. Enter service life of bridge at the end of each year
6. Enter traffic data

Primary calculations

Concrete section

Steel tendon

External load

COMPUTING DATA

Calculate cross sectional area , *Ac*
Calculate second moment of inertia, *I*
Calculate stress at the level of steel, *fc*

Calculate cross-sectional area, Ap
Calculate yield strength, *fpy*
Calculate initial stress in tendon, *fp*
Calculate initial prestressing force, *P*
Calculate eccentricity of the force, *ep*
Calculate eccentricity of tendon lines

Calculate self weight of girder, *Pg*
Calculate Super structure load,*Ps*
Calculate *AADT* and *CESAL*

Prediction of prestress losses at time

Instantaneous (immediate) prestress losses

Long term (time dependent) prestress losses at time *(t)*

| Elastic shortening *(Esh)* | Friction *(Fr)* | Anchorage slip *(As)* | Creep *(CRt)* | Shrinkage *(CRt)* | Relaxation *(REt)* |

Total *IPL*

Total *LPLt*

Loss in prestressing force *LPin*

Total prestress loss *TPLt*

Loss in prestressing force *LPt*

Total loss in prestressing force *TLPt*

Effective prestressing force *EPt*

COMPUTING PRESTRESS LOSSE &FORCES

Fig 3.1 Flow chart

3.10. Data quality assurance

Data collection follows a regular procedure. That means data can be gained from a body having a knowledge and experience on PSC bridge analysis, design and construction. A research is fully dependent on data collected from the following bodies, structural and site engineers, design officers, contactors, and others having knowledge closely related with bridge analysis, design and construction.

3.11. Operational definitions

This research work concludes that though it is impossible to guarantee against fatigue failure yet attempts can be made to increase service life, performance and capacity of bridge under traffic load. The potential causes of fatigue failure can be controlled if proper consideration is given to construction material, analysis, design construction and technique to be used. To predict long term behavior of bridge one should have to review analysis, design and method of construction taken.

CHAPTER FOUR – RESULT AND DISCUSSION

4.1. Introduction

This chapter is mainly focused on description of results obtained from illustrative example. According to this research fatigue due to traffic load and long-term prestress losses are the main factors affecting long term serviceability of PSC Bridge.

In addition to dead loads a bridge is subjected to a large number of cyclic live loads during its operational period. The primary source of these cyclic live loads is traffic vehicle producing fatigue loads. The addition of cyclic live loads to the loading of a bridge introduces the problem of fatigue failure.

Prestress losses are a reduction in the initial prestressing force in the strands (the jacking force) and can be grouped into two general categories, instantaneous losses and long-term losses. Instantaneous losses occur quickly upon release of the tendons and include anchorage slip, elastic shortening, and friction. Time-dependent losses occur more slowly over the life of the bridge and include steel relaxation and concrete creep and shrinkage.

4.2. Results

From this study the following main results can be obtained at different time of prediction.

a) CESAL from traffic analysis
b) Long- term prestress losses
c) Long- term deflection

The details of these results are shown using MATLAB program (Appendix 1 and 2) and MATHCAD PRIME (Appendix 3)

The prediction of these results are based on methods and specifications discussed in literature review (chapter 2)

a) *CESAL is obtained according to traffic analysis*

- $AADT_1 = AADT_0 (1+r)^X$
- $Ti = 365 (P)(D) AADT_{1i} [(1+r_i)^N - 1] / (r_i)$
- $CESAL = \sum(Ti * TFi)$

b) *Instantaneous prestress losses as per N Krishna method*

- Loss due to elastic shortening (Esh)

$$Esh = \alpha \cdot fc$$

- Loss due to friction at mid span (Fr)

$$Fr = fp*(\mu\alpha + Kx)$$

- Loss due to anchorage slips (Asl)

$$Asl = \Delta \cdot Es/L$$

c) *Long term prestress losses as per time step method and N Krishna method*

- loss due to creep of concrete CR at specified time tp

$$CR. (tp) = 0.0285 \cdot fc \cdot (tp-1) \cdot \psi$$

- Loss due to shrinkage of concrete SR at specified time tp

$$SR = (200*10^{-6})/\log (tp+2)$$

- Loss due to relaxation of steel RE at specified time tp

$$RE = \log (24 \cdot tp)/40 *(fp /fpy - 0.55) fp$$

d) *Long term or time dependent deflection as per time step method & N Krishna method*

$$\Delta ntp = \frac{L^2}{8EcI} * (EPtp * ep) + \frac{5L^3}{384EcI}(Pg + Pw + Ptp)$$

         (Upward deflection)   *(Down ward deflection)*

4.3.   Discussion of results

Here the main results under consideration including traffic load analysis, prestress losses and deflection are discussed graphically in relation with time.

1) Traffic load analysis

Traffic analysis studies are conducted in determining the number, movements, and classifications of roadway vehicles at a given location. When a vehicle passes over a bridge it passes a static load along with a dynamic load onto the bridge. The dynamic load is due to the bouncing or vibration effect caused by the interaction between the vehicle's tyres and the bridge's uneven surface. This effect is due to traffic load applied during operational period of the bridge. Hence that traffic load along the route should be conducted to predict long term serviceability behavior of the bridge.

To account for fatigue this study starts from estimation of AADT and traffic volume which serve the important basic data in transportation sector. Traffic is fundamental to the analysis of transportation data sets and the management of transportation systems.

For the route ADAMA –AWASH, traffic data obtained from ERA (central region) is similar to that of MODJO – ADAMA. That means future growth of both route is relatively the same. The following table shows that growth rate of future traffic volumes. As it is shown on the table future growth rate of the traffic volume is predicted only up to 2030, so that prediction for long term serviceability (prestress losses and deflection) is predicted in parallel manner with traffic growth rate

Table 4.1. Growth rate (%) of traffic volumes

Year	Cars	Buses	Trucks
2007-2010	3.5	3.9	4.6
2011-2013	4.6	5.2	6.1
2014-2020	5.8	6.5	7.6
2021-2030	3.5	3.9	4.6

Increment in AADT is closely related with increment of a number of trucks being on the one bridge at a given time, which results in a large static load on the bridge. Along with this increased static load, a bridge also has to react against an imposed dynamic load. The dynamic load increases as the quality of the bridge pavement decreases. Table 4.2 shows future AADT1 predicted up to 2030 based on assigned growth rate. The computation for AADT1 for different type of vehicles is done according to ERADM.

Table 4.2. Future traffic volume estimation

Traffic growth rate				$AADT_1 = AADT_0 (1+r)^x$								
Year	Cars %	Buses %	Trucks %	Car	Land Rover	Small Bus	Large Bus	Small Truck	Medium Truck	Heavy Truck	Truck Trailer	Total
2010	3.5	3.9	4.6	53	288	320	31	242	84	70	1132	2220
2011	4.6	5.2	6.1	55	298	332	32	253	88	73	1184	2316
2012	4.6	5.2	6.1	57	312	350	34	269	93	78	1256	2449
2013	4.6	5.2	6.1	60	326	368	36	285	99	82	1333	2589
2014	5.8	6.5	7.6	63	341	387	37	302	105	87	1414	2737
2015	5.8	6.5	7.6	66	361	412	40	325	113	94	1522	2934
2016	5.8	6.5	7.6	70	382	439	43	350	122	101	1637	3144
2017	5.8	6.5	7.6	74	404	468	45	377	131	109	1762	3369
2018	5.8	6.5	7.6	79	427	498	48	405	141	117	1896	3611
2019	5.8	6.5	7.6	83	452	530	51	436	151	126	2040	3871
2020	5.8	6.5	7.6	88	478	565	55	469	163	136	2195	4149
2021	3.5	3.9	4.6	93	506	602	58	505	175	146	2362	4447
2022	3.5	3.9	4.6	96	524	625	61	528	183	153	2470	4640
2023	3.5	3.9	4.6	100	542	649	63	552	192	160	2584	4842
2024	3.5	3.9	4.6	103	561	675	65	578	201	167	2703	5053
2025	3.5	3.9	4.6	107	581	701	68	604	210	175	2827	5273
2026	3.5	3.9	4.6	111	601	728	71	632	219	183	2957	5502
2027	3.5	3.9	4.6	115	622	757	73	661	230	191	3093	5742
2028	3.5	3.9	4.6	119	644	786	76	692	240	200	3235	5992
2029	3.5	3.9	4.6	123	667	817	79	723	251	209	3384	6253
2030	3.5	3.9	4.6	127	690	849	82	757	263	219	3540	6526

Traffic volume predicts the future service level of the bridge based on the planned traffic volume. In this regard, accurate analysis of traffic data is required to predict serviceability of the bridge and facilitate traffic flow. Once the bridge is opened to traffic, it is subjected to cumulative load from traffic.

According to this study prediction for cumulative traffic volume is started from 2014 and ends at 2030. Actually the bridge illustrated as a representative sample is opened to traffic at the end of 2014, so that the total number of years for prediction is 15. As it is shown on Table 4.3 the future cumulative traffic volume up to 2030 is determined according to ERADM for different type of vehicles.

Table 4.3. Cumulative traffic volume over 15 years

Year	Car	Land Rover	Small Bus	Large Bus	Small Truck	Medium Truck	Heavy Truck	Truck Trailer
2014	479827	2607362	3095092	299837	2588235	898396	748663	12106953
2015	555762	3019992	3638735	352502	3125424	1084858	904048	14619753
2016	587997	3195152	3875253	375415	3362956	1167307	972756	15730854
2017	622101	3380471	4127145	399817	3618541	1256023	1046685	16926399
2018	658182	3576538	4395409	425805	3893550	1351480	1126234	18212805
2019	696357	3783977	4681111	453483	4189460	1454193	1211827	19596978
2020	736746	4003448	4985383	482959	4507859	1564711	1303926	21086348
2021	779477	4235648	5309433	514351	4850456	1683629	1403025	22688911
2022	679054	3689953	4534040	439235	4036307	1401032	1167527	18880575
2023	702821	3819102	4710867	456365	4221977	1465480	1221233	19749081
2024	727420	3952770	4894591	474164	4416188	1532892	1277410	20657539
2025	752879	4091117	5085480	492656	4619332	1603405	1336170	21607786
2026	779230	4234306	5283814	511869	4831822	1677161	1397634	22601744
2027	806503	4382507	5489883	531832	5054085	1754311	1461926	23641424
2028	834731	4535895	5703988	552574	5286573	1835009	1529174	24728929
2029	863946	4694651	5926444	574124	5529756	1919419	1599516	25866460
2030	894184	4858964	6157575	596515	5784124	2007713	1673094	27056317

One vital component in this study is an account for expected magnitude and frequency of traffic loads over the future life of the bridge. Traffic can be characterized using equivalent single axle loads (ESALs). ESALs convert the effect of mixed axle load applications into the equivalent number of applications of 80kN single axle.

Typically, ESALs are calculated per vehicle and then multiplied by the average annual daily traffic (AADT), growth factor, lane distribution, and directional distribution to compute the total ESALs over a given year. The effect of motorcycles, passenger cars, and pick-up trucks on calculation of ESALs per vehicle or the truck factor is very small.

Hence that ESAL per vehicles is determined as per ERADM based on truck equivalency factor provided on Table 2.5.

Table 4.4. ESA per vehicles from 2014-2030

Year	Cars, Land lovers Avg ESA/Veh	ESA	Large Avg ESA/Veh	Bus ESA	Small Avg ESA/Veh	Truck ESA	Medium Avg ESA/Veh	Truck ESA	Heavy Avg ESA/Veh	Truck ESA	Truck Trailer Avg ESA/Veh	ESA
2014	0	0	0.73	0.2	0.7	2	1.7	2	1.8	1.3	2.2	27
2015	0	0	0.73	0.3	0.7	2	1.7	2	1.8	1.6	2.2	32
2016	0	0	0.73	0.3	0.7	2	1.7	2	1.8	1.8	2.2	35
2017	0	0	0.73	0.3	0.7	3	1.7	2	1.8	1.9	2.2	37
2018	0	0	0.73	0.3	0.7	3	1.7	2	1.8	2.0	2.2	40
2019	0	0	0.73	0.3	0.7	3	1.7	2	1.8	2.2	2.2	43
2020	0	0	0.73	0.4	0.7	3	1.7	3	1.8	2.3	2.2	46
2021	0	0	0.73	0.4	0.7	3	1.7	3	1.8	2.5	2.2	50
2022	0	0	0.73	0.3	0.7	3	1.7	2	1.8	2.1	2.2	42
2023	0	0	0.73	0.3	0.7	3	1.7	2	1.8	2.2	2.2	43
2024	0	0	0.73	0.3	0.7	3	1.7	3	1.8	2.3	2.2	45
2025	0	0	0.73	0.4	0.7	3	1.7	3	1.8	2.4	2.2	48
2026	0	0	0.73	0.4	0.7	3	1.7	3	1.8	2.5	2.2	50
2027	0	0	0.73	0.4	0.7	4	1.7	3	1.8	2.6	2.2	52
2028	0	0	0.73	0.4	0.7	4	1.7	3	1.8	2.8	2.2	54
2029	0	0	0.73	0.4	0.7	4	1.7	3	1.8	2.9	2.2	57
2030	0	0	0.73	0.4	0.7	4	1.7	3	1.8	3.0	2.2	60

CESALs per year are obtained from summation of ESAL per vehicles at each year. The future prediction of long term serviceability (loss and deflection) is determined based on CESAL at each year. The equivalent static load of cyclic CESAL at the end of a given year and at the end of a day in the year is obtained as follows.

Table 4.5 CESAL from 2014 to 2030

Year	CESA (10^6)kg	CESAL (kN) Cumulative value	CESAL (kN) Peak value (Year)	CESAL (kN) Peak value (Day)
2014	31.54	315408.08	18116.09	49.63
2015	38.08	380801.25	26717.07	73.20
2016	40.97	409713.84	28912.59	79.21
2017	44.08	440821.94	31108.11	85.23
2018	47.43	474292.30	33470.36	91.70
2019	51.03	510304.33	36012.02	98.66
2020	54.91	549051.04	38746.71	106.16
2021	59.07	590740.14	41689.10	114.22
2022	49.17	491666.23	21555.74	59.06
2023	51.43	514260.43	22594.20	61.90
2024	53.79	537893.09	23632.66	64.75
2025	56.26	562611.94	24718.85	67.72
2026	58.85	588466.92	25854.97	70.84
2027	61.55	615510.24	27043.32	74.09
2028	64.38	643796.53	28286.29	77.50
2029	67.34	673382.94	29586.40	81.06
2030	70.43	704329.22	30946.28	84.78

As it is discussed before AADT along the bridge route is due to traffic volume of different vehicle classification. As vehicles are different type their AADT also increases differently with respect to time. The following graph shows that variation of AADT with time in different vehicles. The graph shows that there is highly increment of AADT in truck trailer and very small increment of AADT in cars, medium truck, large buses and heavy truck.
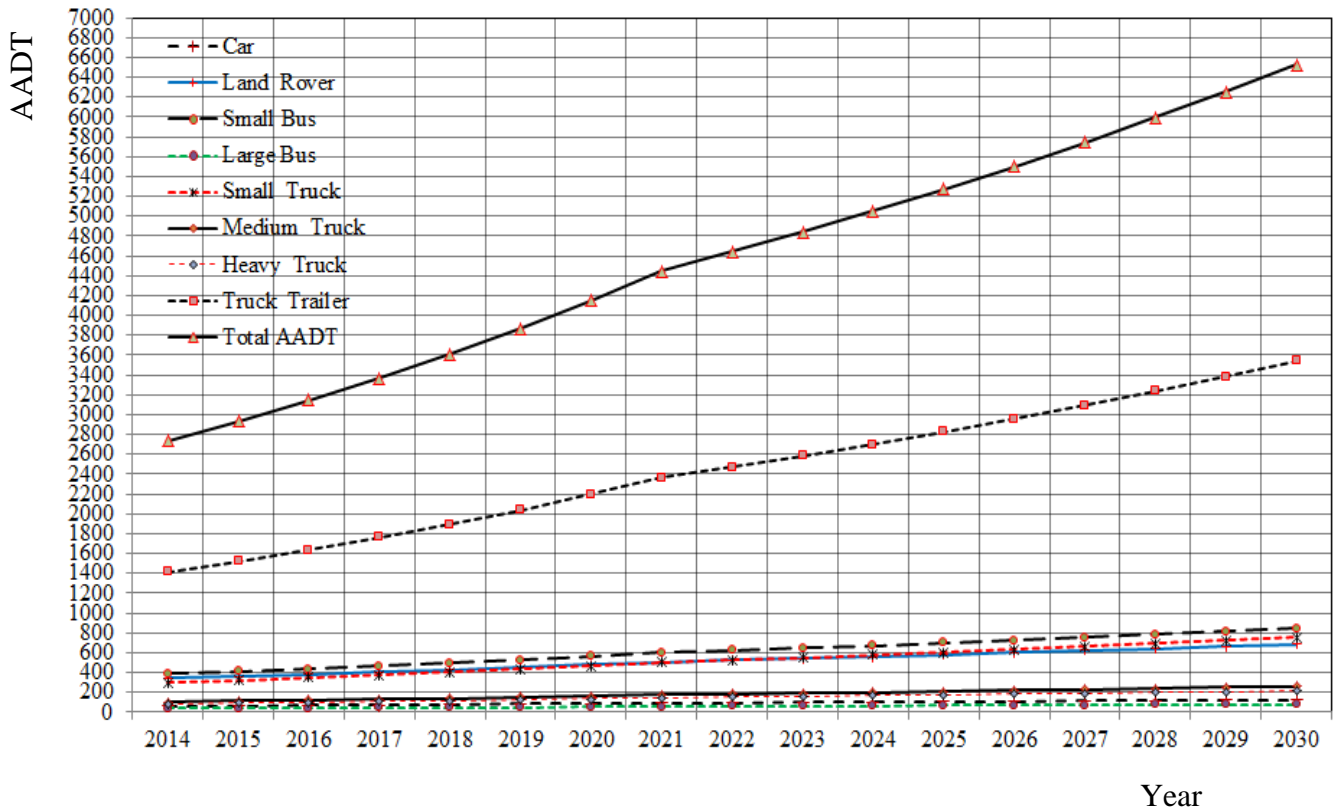

Fig 4.1 Increment of AADT with respect to time (2014-2030)

The corresponding CESAL is fluctuating as cumulative traffic volume is changed from year to year. Here the cumulative CESAL at the end of the year and peak value of CESAL for individual year are shown. Cumulative CESAL is rapidly increasing up to 2021 and it becomes decreases due to decrease in growth rate of traffic volume after 2021. In the same way the peak value of CESAL at individual year is slowly increasing similar to the cumulative CESAL and decreases due to decrease in growth rate of traffic volume after 2021.
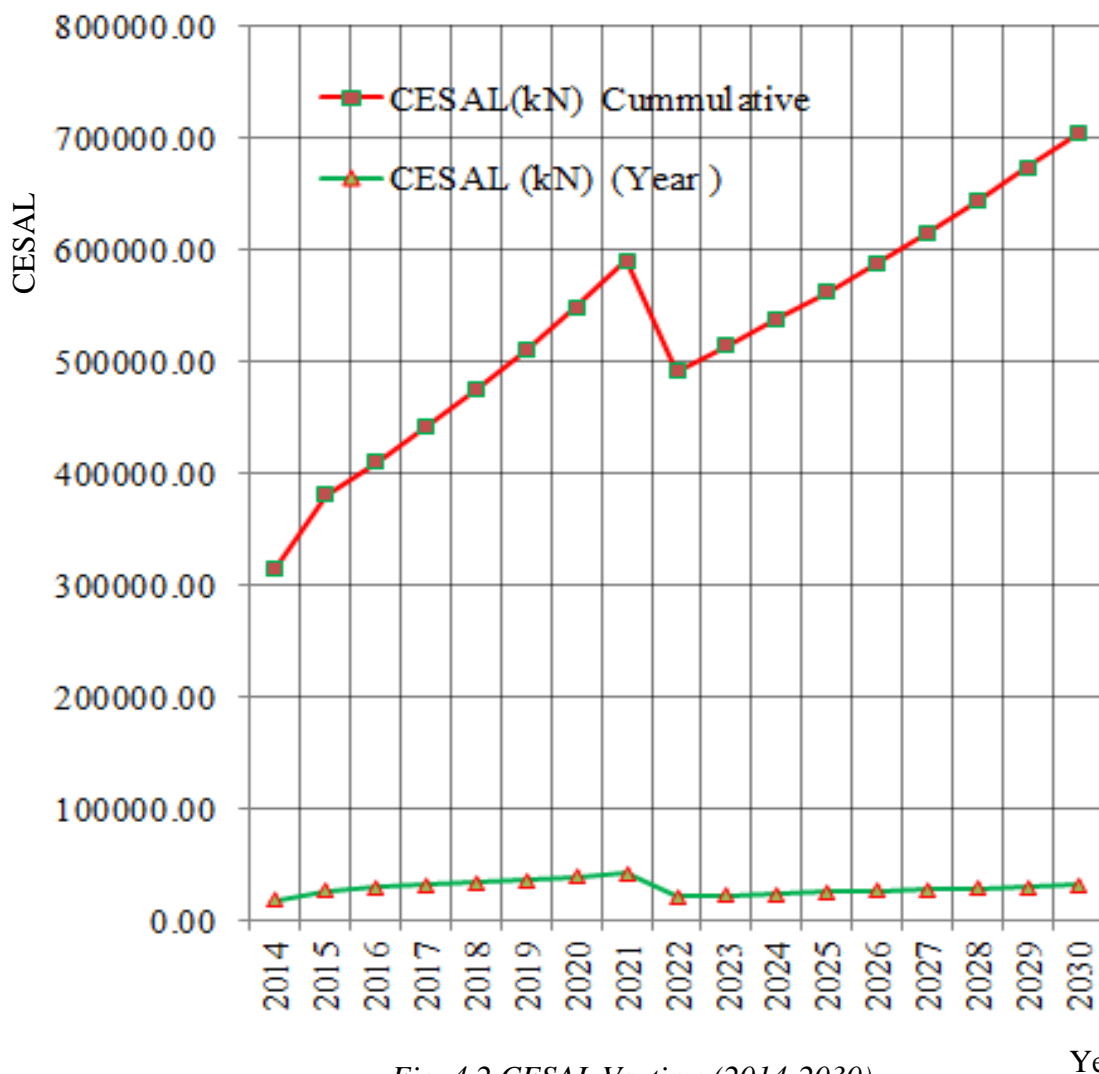
Fig. 4.2. CESAL Vs. time (2014-2030)

2) Long term prestress losses

Creep and shrinkage of concrete and relaxation of prestressing steel cause time dependent changes in the stresses and strains of concrete structures. These changes result in continuous reduction in the concrete compression stresses and in the tension in prestressing steel.

The effects of these factors are interdependent and it is usually difficult to isolate the effect of each factor. While it is generally accepted that long-term losses do not affect the ultimate capacity of a prestressed concrete member, a reasonably accurate prediction of long-term losses is important to ensure satisfactory performance of the PSC Bridge under service loads.

If prestress losses are underestimated, the tensile strength of concrete could be exceeded at critical sections (mid-spans and over supports) under full service loads and thereby causing cracking and large deflections. On the other hand, overestimating prestress losses leads to excessive camber and uneconomic design because of using large amounts of prestressing steel.

According to this study accurate estimate of the long-term prestress losses are needed to predict long term serviceability behavior (excessive deflection) of the bridge. Different method and specifications are studied to predict the long-term prestress losses in PSC Bridge. The predictions of the proposed method are compared with the current provisions of design standards and codes of practice.

Creep of concrete is the increase of strain under sustained stress. This increase in strain can be several times the elastic (or instantaneous) strain at first loading. As curing of concrete ends, concrete starts to lose moisture and undergoes change in volume as a result of chemical reactions between cement paste and water. This phenomenon is known as shrinkage and it starts to develop rapidly after time t. In PSC Bridge, the two ends of the prestressing tendons constantly move toward each other because of the creep and shrinkage effects of concrete, thereby reducing the tensile stress in the tendons. This reduction in tension has a similar effect as if the tendons were subjected to lesser initial stress.

Change in volume due to creep and shrinkage and relaxation are causes for loss in pre stress. But the variation with time in loss due to creep, shrinkage and relaxation is quietly different as shown Fig 4.5 below.

As shown on fig 4.5 the graph for long term prestress losses (LPL) reflects different behaviors. The graph for long term shrinkage and relaxation loss vary slowly because these graphs are that of logarithmic functions varying with time and show small variation from year to year. The graph for long term creep and total loss vary rapidly because these graphs are that of linear functions varying with time and load. LPL is a function of loss due to creep, shrinkage and relaxation with respect to time.

In this prediction time (2014-2030) percentage loss due to creep is rapidly increasing from 0-61% and loss due to shrinkage is slowly decreasing from 84-21%. Loss due to relaxation of steel is slowly increasing up to 2017 (16-29%) and decreasing slowly after 2017 (29-18%)
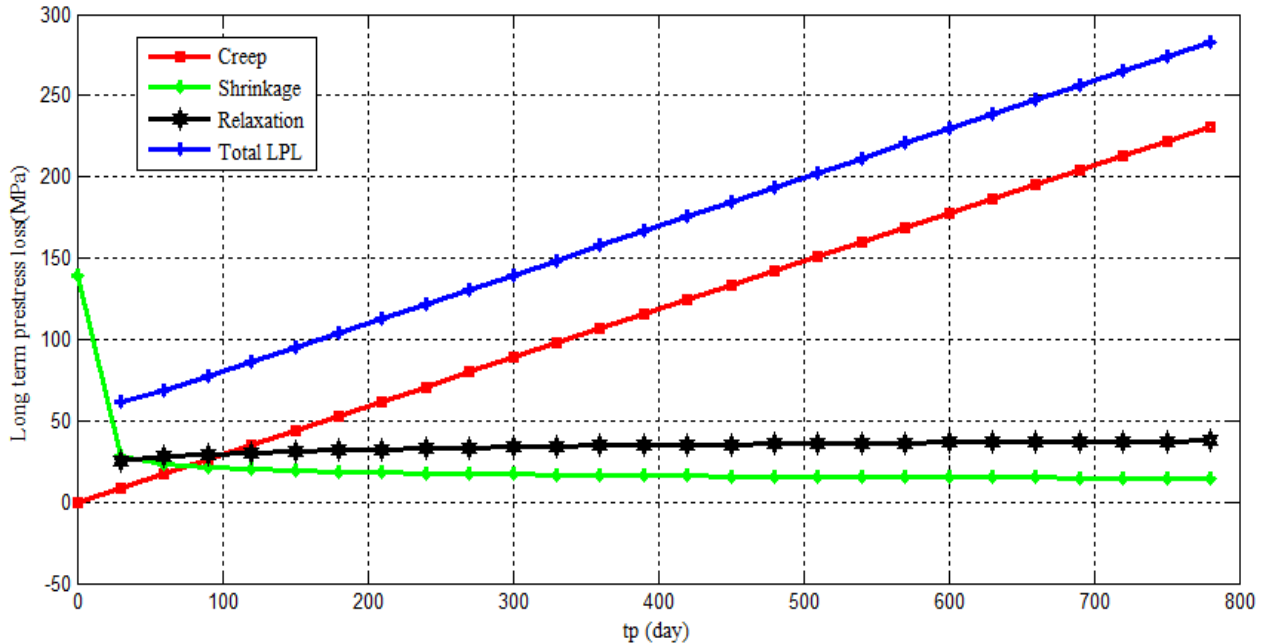
Fig. 4.3.   Fig 8.3 Time Vs Long term prestres losses

Long term loss in prestress force (LP) is obtained from multiplication of total long term prestress losses by total area of rebars provided. The property of LP is the same with LPL because graph for LP is obtained by multiplying LPL function with constant value of total area of rebars provided. The graph for long term loss in prestress force (LP) varies from year to year as shown below.
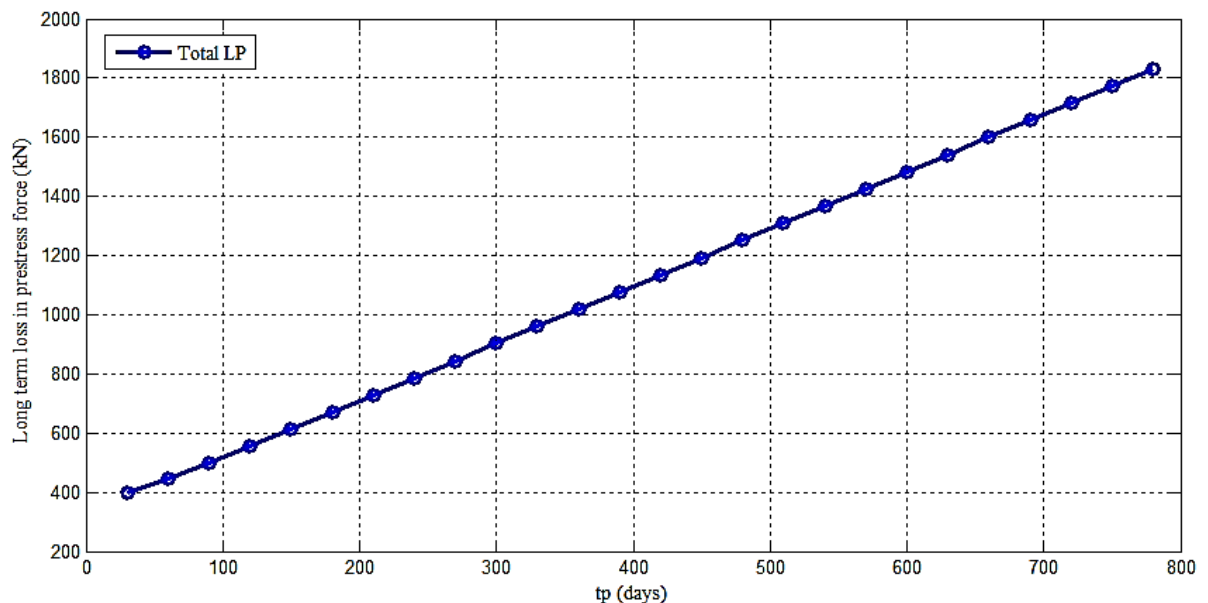

Fig. 4.4.   Time Vs Long term loss in prestress force

Total prestress loss (TPL) is a combination of instantaneous loss (elastic shortening, friction and slip) and long term losses (creep, shrinkage and relaxation of steel). TPL for the specified prediction time is rapidly increasing from year to year. Behavior of TPL up to 2016 (760 days) is shown below.
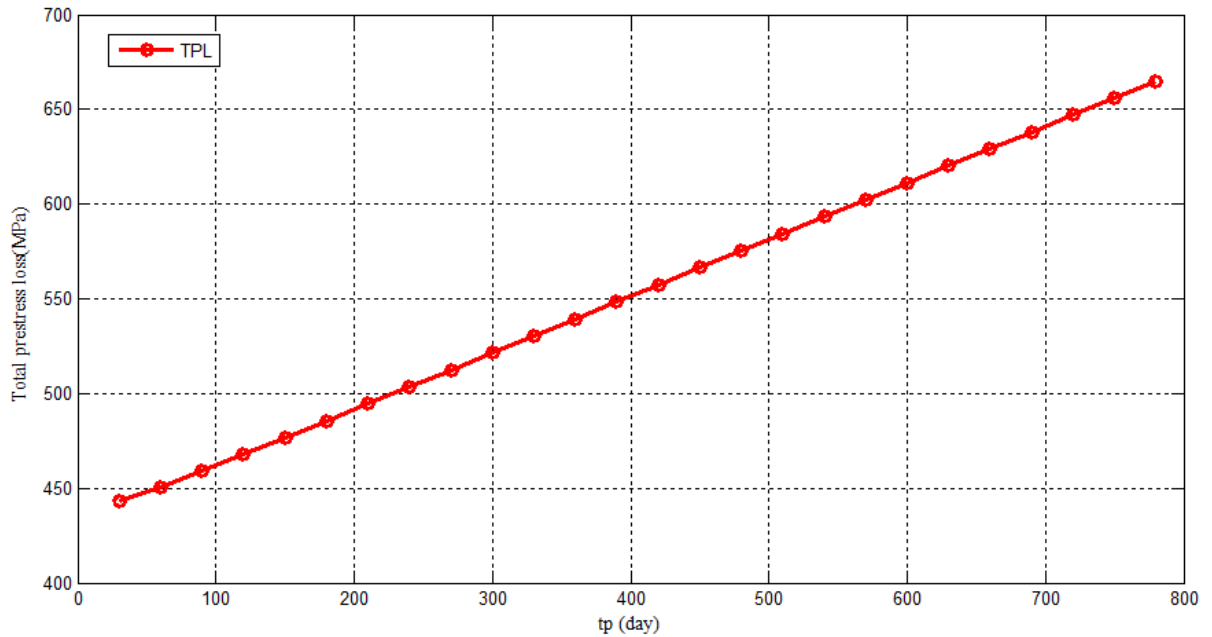

Fig. 4.5. . *Time Vs Total prestress loss*

Total loss in prestress force (TLP) is a combination of loss in force at instantaneous and long term stages. Effective prestress force (EP) is the remaining amount of prestress force after a given loss. So that TLP and EP are the two opposing functions with each other's as show below. The graph shows that rapid increment of TLP and rapid decrease in EP with in specified prediction of time.
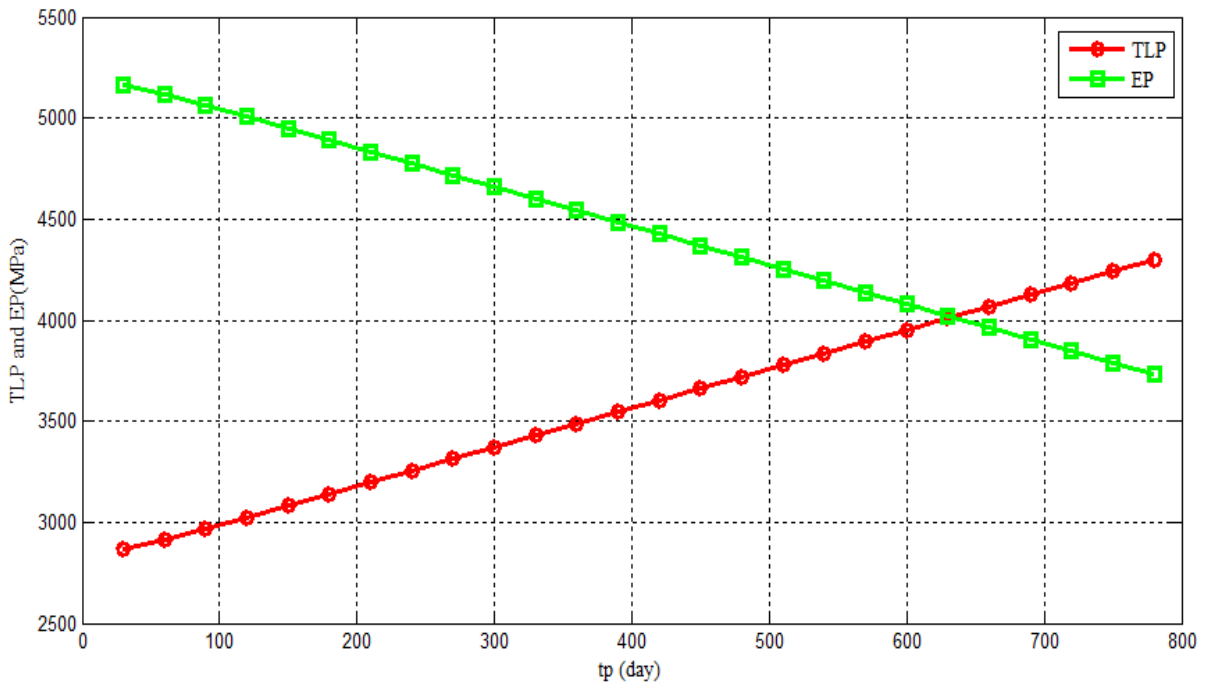

Fig. 4.6.   *Time Vs (Total loss in prestressing force and effective prestress force)*

Generally increment of long term losses starting from 2014 – 2030 is generalized on table 4.7. As it is shown from the table increment in percentage of loss due to creep is greater than that of shrinkage and relaxation. That means loss due to creep is governing factor in long term prestress loss of the bridge.

Table 4.6.Cumulative long term prestress losses: from 2014 to 2030

Year	CR(MPa)	SR(MPa)	RE(MPa)	LPL(MPa)	%ge of CR	%ge of SR	%ge of RE
2014	0.16	27.90	5.28	33.35	0	84	16
2015	2.39	44.06	12.63	59.09	4	75	21
2016	6.52	30.73	15.22	52.48	12	59	29
2017	10.65	28.34	16.06	55.05	19	51	29
2018	14.78	27.00	16.60	58.37	25	46	28
2019	18.90	26.08	17.00	61.99	30	42	27
2020	23.03	25.40	17.32	65.75	35	39	26
2021	27.16	24.86	17.59	69.61	39	36	25
2022	31.29	24.41	17.82	73.51	43	33	24
2023	35.41	24.03	18.02	77.46	46	31	23
2024	39.54	23.71	18.20	81.45	49	29	22
2025	43.67	23.42	18.36	85.45	51	27	21
2026	47.80	23.17	18.50	89.47	53	26	21
2027	51.93	22.94	18.63	93.50	56	25	20
2028	56.05	22.73	18.76	97.54	57	23	19
2029	60.18	22.54	18.87	101.60	59	22	19
2030	64.31	22.37	18.98	105.66	61	21	18

3) Long term deflection

Long term deflection is due to prestress losses, self-weight of the member and CESAL. Deflection result is both upward (camber) by prestress force and down ward by gravitational loads as shown below. As shown on the figure the graph for net deflection is close to graph for upward deflection, which means upward deflection is governing up to 2030. Because effective prestress force at the end of each year is greater than gravitational load from self-weight, wearing surface and CESAL.

Fig 4.7 time Vs deflection
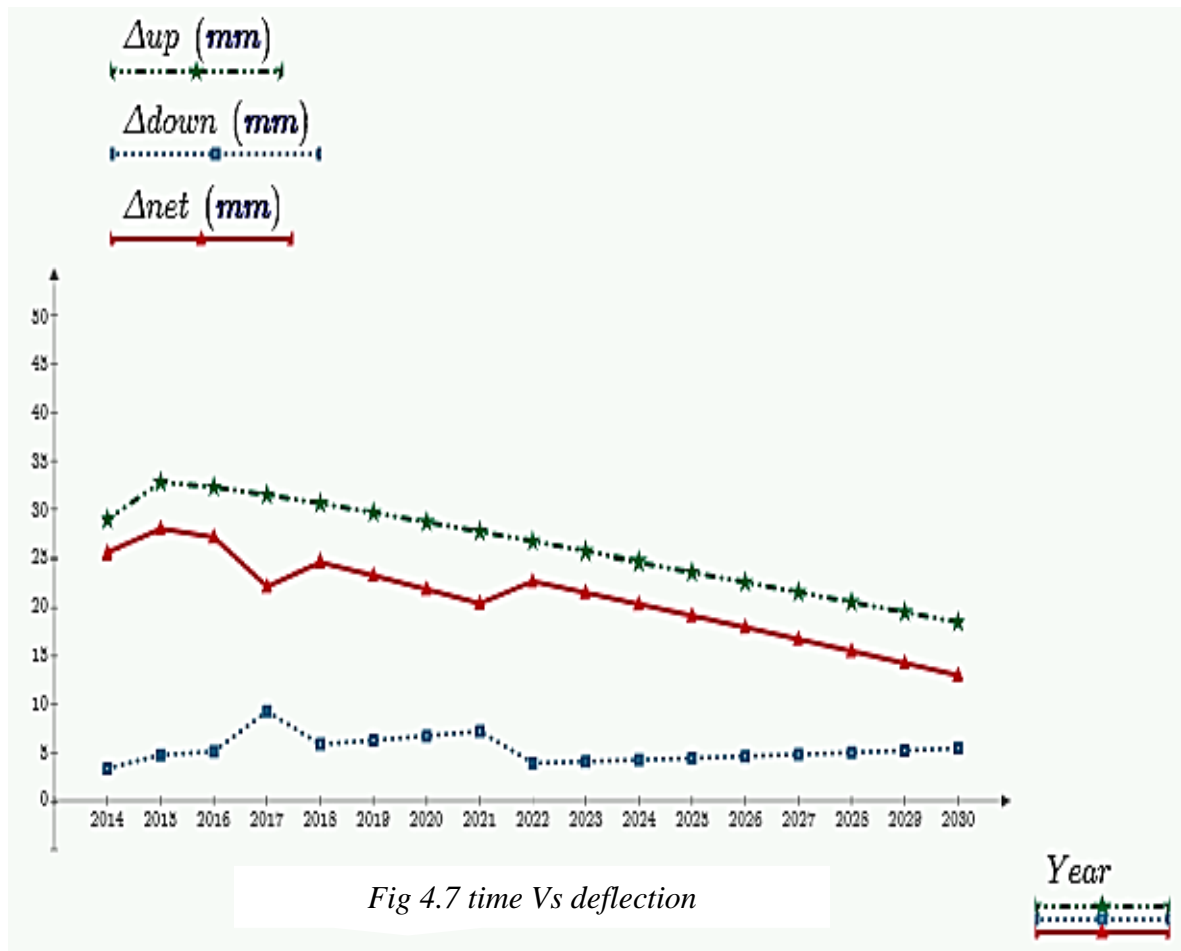
Table 4.7. Predicted deflection results from 204-2030

Year	EP at layer (N)	Δ_{up} (mm)	Δ_{down} (mm)	Δ_{net} (mm)	Comment		Year	EP at layer (N)	Δ_{up} (mm)	Δ_{down} (mm)	Δ_{net} (mm)	Comment
2014	7.83E+05	28.94	3.40	25.54	Upward		2023	6.96E+05	25.70	4.13	21.57	Upward
	1.10E+06							9.73E+05				
	3.28E+05							2.91E+05				
	9.96E+05							8.85E+05				
2015	8.87E+05	32.81	4.81	28.00	Upward		2024	6.69E+05	24.68	4.30	20.38	Upward
	1.24E+06							9.35E+05				
	3.73E+05							2.79E+05				
	1.13E+06							8.50E+05				
2016	8.74E+05	32.30	5.16	27.13	Upward		2025	6.41E+05	23.66	4.48	19.18	Upward
	1.22E+06							8.96E+05				
	3.67E+05							2.68E+05				
	1.11E+06							8.15E+05				
2017	8.52E+05	31.50	5.52	25.98	Upward		2026	6.13E+05	22.64	4.67	17.98	Upward
	1.19E+06							8.57E+05				
	3.58E+05							2.56E+05				
	1.08E+06							7.80E+05				
2018	8.28E+05	30.61	5.91	24.70	Upward		2027	5.86E+05	21.61	4.86	16.76	Upward
	1.16E+06							8.18E+05				
	3.47E+05							2.44E+05				
	1.05E+06							7.44E+05				
2019	8.03E+05	29.66	6.32	23.34	Upward		2028	5.58E+05	20.59	5.06	15.52	Upward
	1.12E+06							7.79E+05				
	3.37E+05							2.32E+05				
	1.02E+06							7.09E+05				
2020	7.77E+05	28.69	6.77	21.92	Upward		2029	5.30E+05	19.55	5.27	14.28	Upward
	1.09E+06							7.40E+05				
	3.25E+05							2.20E+05				
	9.88E+05							6.73E+05				
2021	7.50E+05	27.71	7.25	20.46	Upward		2030	5.02E+05	18.52	5.50	13.03	Upward
	1.05E+06							7.01E+05				
	3.14E+05							2.09E+05				
	9.54E+05							6.38E+05				
2022	7.23E+05	26.71	3.96	22.74	Upward							
	1.01E+06											
	3.03E+05											
	9.20E+05											

CHAPTER FIVE- CONCLUSION AND RECOMMENDATION

5.1. Conclusion

The long-term behavior of PSC bridges is a time dependent function closely related to the following parameters i.e. design output, fatigue load from traffic flow, Creep of concrete shrinkage of concrete, relaxation of steel and time.

- According to this research total LPL at 2030 is largely affected by creep of concrete (61%) which is varied rapidly because it is a linear function varying with time and load. Shrinkage of concrete (21%) and relaxation of steel (18%) do not as much vary as creep of concrete in relation with time because these parameters are that of logarithmic functions varying with time and show small variation from year to year.
- Long term deflection of a bridge is a combination of upward deflection or camber by effective prestress force and downward deflection by sustained dead load and CESAL.
- Here what I want to conclude is that the gradual variation of CESAL from year to year is relatively small and it is followed by relatively similar downward deflection of a bridge. But the actual deflection of the bridge is more dependent on prestress loss. That means the net deflection is governed by deflection due to prestress loss up to 2030. Because effective prestress force at the end of each year is greater than gravitational load from self-weight, wearing surface and CESAL.
- So that fatigue load due to traffic data along the bridge route has no significant effect on serviceability of bridge up to 2030
- Further study should be taken to determine governing factors which affect long term serviceability of the bridge

5.2. Recommendation

This research is closely related with traffic load and time constraint. Here what I want to recommend for future researcher is that;

➢ How to predict long term serviceability behavior and service life of a cracked PSC bridge under different environmental conditions, fatigue load and time.

➢ The effects of the strand temperature on the prestressing force should be analyzed in further detail.

➢ The effect of void deformation with respect to the flexural performance and limit-states of the PSC Bridge.

REFERENCES

1. American Association of State Highway and Transportation Officials (AASHTO), Load Resistance Factored Design (LRFD) Bridge Design Specification, (2004 and 2005)

2. Federal Democratic Republic of Ethiopia, Ethiopian Roads Authority: Bridge Design Manual, Addis Ababa (2002)

3. PCI(pre stressed concrete institute) hand book 5th edition

4. ACI(American concrete institute), Prediction of long term prestress losses (2002)

5. NCHRP(National Cooperative Highway Research Program) hand book

6. Abrham, G. Master's thesis, computer program for comparative study of the analysis and design of Slab and T- girder bridges.(2006)

7. Tewodros, T. Master's thesis, software development for design of Slab and T-girder reinforced concrete bridges.(2009)

8. Highway engineering handbooks

9. Mohsen Heshmati. Fatigue life assessment of the bridge.(2012)

10. Franklin, B. Angomas. Behavior of PSC Bridge Girders. (2009)

11. N Krishna, R. Pre stressed concrete structures, 4th edition

12. Christopher J. Waldron, Investigation of long-term pre stress losses in pre tensioned high performance concrete girders, (2004)

13. R.I.Gilbert and N.C.Mick Leborough, Design of Pre stressed Concrete (1990)

14. Paul W. Ables, Introduction to Pre stressed Concrete vol1&2(1964)

15. T.Y.Lin and NedH.Burns, Design of Pre stressed Concrete Structures (1982) (3rdEdition)

16. H.Kent Preston and Noman J.Sollenberger, Modern Pre stressed Concrete (1967)

17. James R.Libby, Modern Pre stressed Concrete (1971)

18. C.Menn, Pre stressed Concrete Bridges (1990)

19. Firtz Leonhardt, Pre stressed Concrete Design and Construction (1964)

20. Ben C. Gerwick, JR., Construction of Pre stressed Concrete Structures (2nd edition)

21. R.J.Cope, Performance and Advances of Bridge, Concrete Bridge Engineering, Elsevier Applied Science Publishers Ltd., London(2004)

22. Wai-Fah Bridge, Engineering Handbook, CRC Press, USA, (2002)

APPENDICES

Appendix 1 MATLAB program

```
%MATLAB program written to predict long-term service ability behavior of PSC Box Girder Bridge
%Prediction of long-term prestress losses and forces
%Prediction of long term deflection
%The case of PSC Box Girder Bridge over Awash River
%Total span length of 145m
%Span under consideration is interior one with single cell Box Girder

%Material properties
fck=31;%Enter compressive strength of concrete in MPa
Ec=31.5*10^3;%Enter modulus of elasticity of concrete in MPa
Gamma =2.5*10^-5;%Enter unit weight of concrete in N/mm^3
fyd=347.83;%Enter ultimate tensile strength of steel tendons in MPa
Es=210*10^3;%Enter modulus of elasticity of concrete in MPa

%Design out put
NL=6;%Enter total number of layers of rebars
y1=34;y2=216;y3=510;y4=35;y5=245;y6=490;%Enter location of rebars from the face of bottom and top
slab
Phi1=16;Phi2=16;Phi3=19;Phi4=13;Phi5=13;Phi6=19;%Enter diameter of single rebar at each layers in
mm
NR1=68;NR2=68;NR3=68;NR4=44;NR5=132;NR6=68;%Enter number of rebars at each layers
%Enter width of girder, thickness of web, thickness of flanges, depth of girder and length of the span in
mm
be=5400;bw=400;ht=280;hb=250;D=2000;L=70000;
Dw=1.1;%Enter uniform dead load from wearing surface obtained from analysis output in kN/m^2
Miw=0.35;%Enter coefficient of friction between cable and duct
K=1.5*10^-6;%Enter friction coefficient for wave effect in 1/mm
Delta=5;%Enter observed slip at the jacking end in mm
H=35;%Enter Relative humidity of the area
Psi=0.018;%Enter creep coefficient for specified relative humidity
t=760;%Enter time at each predictions to be taken in days (take the end of 2016)
tmax=15;%Enter maximum time of prediction in years
%Enter Bridge service life from traffic opening to maximum time of prediction in days (from Dec 2014 to
end of 2030)
to=0;t14=to+30,t15=t14+365,t16=t15+365,t17=t16+365,t18=t17+365,t19=t18+365,
t20=t19+365,t21=t20+365,t22=t21+365,t23=t22+365,t24=t23+365,t25=t24+365,
t26=t25+365,t27=t26+365,t28=t27+365,t29=t28+365,t30=t29+365,
%Enter average cumulative gravitational load in a day due to CESAL at the end of each years
P14=49630;P15=73200;P16=79210;P17=85230;P18=91700;P19=98660;P20=106160;
P21=114220;P22=59060;P23=61900;P24=64750;P25=67720;P26=70840;P27=74090;
P28=77500;P29=81060;P30=84780;

%Primary calculations
%Calculate cross sectional area of girder in mm^2
Ac=(be*ht)+(2*bw*(D-ht-hb))+(be*hb)
%Calculate location of center of gravity of the girder from the bottom in mm
Yc=[(be*hb*hb/2)+2*(D-hb-ht)*bw*(hb+(D-hb-ht)/2)+(be*ht*(D-ht/2))]/[(be*ht)+(2*bw*(D-ht-
hb))+(be*hb)],
%Calculate second moment of inertia of the girder about Yc in mm^4
I1=(be*hb^3)/12+be*hb*(Yc-hb/2)^2,I2=(bw*(D-ht-hb)^3)/12+bw*(D-ht-hb)*(hb+(D-hb-ht)/2-
Yc)^2,I3=I2,
```

I4=(be*ht^3)/12+be*ht*(Yc-(D-ht/2))^2,I=I1+I2+I3+I4,

%Calculate cross sectional area of single rebar at each layer in mm^2
As1=(pi*Phi1^2)/4,As2=(pi*Phi2^2)/4,As3=(pi*Phi3^2)/4,As4=(pi*Phi4^2)/4,As5=(pi*Phi5^2)/4,As6=(pi*Phi6^2)/4,
%Calculate total cross sectional area of rebars at each layers in mm^2
Ap1=NR1*As1,Ap2=NR2*As2,Ap3=NR3*As3,Ap4=NR4*As4,Ap5=NR5*As5,Ap6=NR6*As6,Ap=Ap1+Ap2+Ap3+Ap4+Ap5+Ap6,
%Calculate yield strength of rebar in MPa, initial stress in MPa, initial prestressing force at each layers in N
fpy=0.9*fyd,fp=0.75*fyd,P1=fp*Ap1,P2=fp*Ap2,P3=fp*Ap3,P4=fp*Ap4,P5=fp*Ap5,P6=fp*Ap6,P=P1+P2+P3+P4+P5+P6,
%Calculate self-weight of the girder and mid span load by wearing surface in N
Pg=Ac*L/1000*Gamma,Pw=Dw*be*L/1000^2,
%Calculate location of prestressing force from the bottom and eccentricity of prestressing force from girder centroid in mm
Y=(Ap1*y1+Ap2*y2+Ap3*y3+Ap4*y4+Ap5*y5+Ap6*y6)/Ap,ep=Yc-Y,
%Calculate eccentricity of location of rebar profile at each layers and average eccentricity from the girder centroid in mm
e1=Yc-y1,e2=Yc-y2,e3=Yc-y3,e4=D-Yc-y4,e5=D-Yc-y5,e6=D-Yc-y6,yb=(e1+e2+e3+e4+e5+e6)/6,
%Calculate cumulative angle in radian in which the tangent to the rebar profile has turned
Alpha1=0,Alpha2=0,Alpha3=0,Alpha4=0,Alpha5=0,Alpha6=0,%Because all layers are straight rebars
%Calculate modular ratio and stress in the concrete at the level of steel in MPa
Alpha=Es/Ec,fc=P/Ac+(P*ep*yb)/I,

%Instantaneous or Immediate prestress losses%
%Calculate loss due to elastic shortening, friction and anchorage slip and total instantaneous prestress loss in MPa
x=L/2,Esh=Alpha*fc,Fr=6*fp*(Miw*Alpha1+K*x),Asl=Delta*Es/L,IPL=Esh+Fr+Asl,
%Calculate loss in prestressing force at each layers and total loss in prestressing force due to instantaneous losses in N
LP1=IPL*Ap1,LP2=IPL*Ap2,LP3=IPL*Ap3,LP4=IPL*Ap4,LP5=IPL*Ap5,LP6=IPL*Ap6,LPin=IPL*Ap,

%Long-term or time dependent prestress losses%
%Calculate loss due to creep, shrinkage, relaxation and total long-term prestress loss in MPa and total long-term loss in prestressing force in N at specified time
CR=0.0285*fc*(t-1)*Psi,SR=200*10^-6*Es/log10(t+2), RE=log10(24*t)*(fp/fpy-0.55)*fp/40,LPLt=CR+SR+RE,LPt=LPLt*Ap,
%Calculate total prestress loss in MPa and total loss of prestressing force at specified time
TPLt=IPL+LPLt,TLPt=LPin+LPt,
%Calculate effective prestress force at each layer and total effective prestress force in N at specified time
EPt1=P1-(LP1+(0.0285*fc*(t-1)*Psi+200*10^-6*Es/log10(t+2)+log10(24*t)*(fp/fpy-0.55)*fp/40)*Ap1),
EPt2=P2-(LP2+(0.0285*fc*(t-1)*Psi+200*10^-6*Es/log10(t+2)+log10(24*t)*(fp/fpy-0.55)*fp/40)*Ap2),
EPt3=P3-(LP3+(0.0285*fc*(t-1)*Psi+200*10^-6*Es/log10(t+2)+log10(24*t)*(fp/fpy-0.55)*fp/40)*Ap3),
EPt4=P4-(LP4+(0.0285*fc*(t-1)*Psi+200*10^-6*Es/log10(t+2)+log10(24*t)*(fp/fpy-0.55)*fp/40)*Ap4),
EPt5=P5-(LP5+(0.0285*fc*(t-1)*Psi+200*10^-6*Es/log10(t+2)+log10(24*t)*(fp/fpy-0.55)*fp/40)*Ap5),
EPt6=P6-(LP6+(0.0285*fc*(t-1)*Psi+200*10^-6*Es/log10(t+2)+log10(24*t)*(fp/fpy-0.55)*fp/40)*Ap6),
EPt=P-TLPt,
%Plot the graph for time dependent prestress losses with respect to time of prediction
subplot(4,2,1);
tp=0:30:780;CR=0:50:300,SR=0:50:300,RE=0:50:300,LPL=0:50:300
CR=0.0285*fc*(tp-1)*Psi;SR=200*10^-6*Es./log10(tp+2);RE=log10(24*tp)*(fp./fpy-0.55)*fp./40
LPL=0.0285*fc*(tp-1)*Psi+200*10^-6*Es./log10(tp+2)+log10(24*tp)*(fp./fpy-0.55)*fp/40
plot(tp,CR,tp,SR,tp,RE,tp,LPL)
plot(tp,CR,'r',tp,SR,'g',tp,RE,'k',tp,LPL,'b','linewidth',2)

```
axis tight
xlabel('tp (day)')
ylabel('Long term prestress loss(MPa)')
title('Time Vs Long term prestres losses')
legend('Creep','Shrinkage','Relaxation','Total LPL')
%Plot the graph for total long-term loss in prestressing force with respect to time of prediction
subplot(4,2,2);
tp=0:30:780;LP=0:500:5000
LP=(0.0285*fc*(tp-1)*Psi+200*10^-6*Es./log10(tp+2)+log10(24*tp)*(fp./fpy-0.55)*fp/40)*Ap
plot(tp,0.001*LP)
plot(tp,0.001*LP,'r','linewidth',2)
axis tight
xlabel('tp (days)')
ylabel('Long term loss in prestress force (kN)')
title('Time Vs Long term loss in prestress force')
legend('Total LP')
%Plot the graph for total prestress loss with respect to time of prediction
subplot(4,2,3);
tp=0:30:780;TPL=0:100:1000
TPL=IPL+0.0285*fc*(tp-1)*Psi+200*10^-6*Es./log10(tp+2)+log10(24*tp)*(fp./fpy-0.55)*fp/40
plot(tp,TPL)
plot(tp,TPL,'b','linewidth',2)
axis tight
xlabel('tp (day)')
ylabel('Total prestress loss(MPa)')
title('Time Vs Total prestress loss')
legend('TPL')
%Plot the graph for total loss in prestressing force and total effective prestress force with respect to time of
prediction
subplot(4,2,4);
tp=0:30:780;TLP=0:500:6000;EP=0:500:6000
TLP=LPin+(0.0285*fc*(tp-1)*Psi+200*10^-6*Es./log10(tp+2)+log10(24*tp)*(fp./fpy-0.55)*fp/40)*Ap
EP=P-(LPin+(0.0285*fc*(tp-1)*Psi+200*10^-6*Es./log10(tp+2)+log10(24*tp)*(fp./fpy-0.55)*fp/40)*Ap)
plot(tp,0.001*TLP,tp,0.001*EP)
plot(tp,0.001*TLP,'r',tp,0.001*EP,'g','linewidth',2)
axis tight
xlabel('tp (day)')
ylabel('TLP and EP(MPa)')
title('Time Vs (Total loss in prestressing force and effective prestress force)')
legend('TLP','EP')

%Long-term or time dependent deflection)
%Deflection at the end of 2014
%calculate total effective prestress force at each layers at the end of 2014 in kN
EP14_1=P1-(LP1+(0.0285*fc*(t14-1)*Psi+200*10^-6*Es/log10(t14+2)+log10(24*t14)*(fp/fpy-
0.55)*fp/40)*Ap1)
EP14_2=P2-(LP2+(0.0285*fc*(t14-1)*Psi+200*10^-6*Es/log10(t14+2)+log10(24*t14)*(fp/fpy-
0.55)*fp/40)*Ap2)
EP14_3=P3-(LP3+(0.0285*fc*(t14-1)*Psi+200*10^-6*Es/log10(t14+2)+log10(24*t14)*(fp/fpy-
0.55)*fp/40)*Ap3)
EP14_4=P4-(LP4+(0.0285*fc*(t14-1)*Psi+200*10^-6*Es/log10(t14+2)+log10(24*t14)*(fp/fpy-
0.55)*fp/40)*Ap4)
EP14_5=P5-(LP5+(0.0285*fc*(t14-1)*Psi+200*10^-6*Es/log10(t14+2)+log10(24*t14)*(fp/fpy-
0.55)*fp/40)*Ap5)
EP14_6=P6-(LP6+(0.0285*fc*(t14-1)*Psi+200*10^-6*Es/log10(t14+2)+log10(24*t14)*(fp/fpy-
0.55)*fp/40)*Ap6)
```

%Calculate cumulative upward deflection (camber) by EP in straight rebar in mm
Dup_14=L^2*(EP14_1*e1+EP14_2*e2+EP14_3*e3+EP14_4*e4+EP14_5*e5+EP14_6*e6)/(8*Ec*I)
%Calculate cumulative downward deflection by self-weight of girder, wearing surface and CESAL in mm
Ddown_14=5*L^3*(Pg+Pw+P14)/(384*Ec*I)
%Calculate net deflection in mm
Dnet_14=Dup_14-Ddown_14

%Deflection at the end of 2015
%calculate total effective prestress force at each layers at the end of 2015 in kN
EP15_1=P1-(LP1+(0.0285*fc*(t15-1)*Psi+200*10^-6*Es/log10(t15+2)+log10(24*t15)*(fp/fpy-0.55)*fp/40)*Ap1),EP15_2=EP15_1
EP15_3=P3-(LP3+(0.0285*fc*(t15-1)*Psi+200*10^-6*Es/log10(t15+2)+log10(24*t15)*(fp/fpy-0.55)*fp/40)*Ap3)
EP15_4=P4-(LP4+(0.0285*fc*(t15-1)*Psi+200*10^-6*Es/log10(t15+2)+log10(24*t15)*(fp/fpy-0.55)*fp/40)*Ap4)
EP15_5=P5-(LP5+(0.0285*fc*(t15-1)*Psi+200*10^-6*Es/log10(t15+2)+log10(24*t15)*(fp/fpy-0.55)*fp/40)*Ap5),EP15_6=EP15_3
%Calculate cumulative upward deflection (camber) by EP in straight rebar in mm
Dup_15=L^2*(EP15_1*e1+EP15_2*e2+EP15_3*e3+EP15_4*e4+EP15_5*e5+EP15_6*e6)/(8*Ec*I)
%Calculate cumulative downward deflection by self-weight of girder, wearing surface and CESAL in mm
Ddown_15=5*L^3*(Pg+Pw+P15)/(384*Ec*I)
%Calculate net deflection in mm
Dnet_15=Dup_15-Ddown_15

%Deflection at the end of 2016
%calculate total effective prestress force at each layers at the end of 2016 in kN
EP16_1=P1-(LP1+(0.0285*fc*(t16-1)*Psi+200*10^-6*Es/log10(t16+2)+log10(24*t16)*(fp/fpy-0.55)*fp/40)*Ap1),EP16_2=EP16_1
EP16_3=P3-(LP3+(0.0285*fc*(t16-1)*Psi+200*10^-6*Es/log10(t16+2)+log10(24*t16)*(fp/fpy-0.55)*fp/40)*Ap3)
EP16_4=P4-(LP4+(0.0285*fc*(t16-1)*Psi+200*10^-6*Es/log10(t16+2)+log10(24*t16)*(fp/fpy-0.55)*fp/40)*Ap4)
EP16_5=P5-(LP5+(0.0285*fc*(t16-1)*Psi+200*10^-6*Es/log10(t16+2)+log10(24*t16)*(fp/fpy-0.55)*fp/40)*Ap5),EP16_6=EP16_3
%Calculate cumulative upward deflection (camber) by EP in straight rebar in mm
Dup_16=L^2*(EP16_1*e1+EP16_2*e2+EP16_3*e3+EP16_4*e4+EP16_5*e5+EP16_6*e6)/(8*Ec*I)
%Calculate cumulative downward deflection by self-weight of girder, wearing surface and CESAL in mm
Ddown_16=5*L^3*(Pg+Pw+P16)/(384*Ec*I)
%Calculate net deflection in mm
Dnet_16=Dup_16-Ddown_16

%Deflection at the end of 2017
%calculate total effective prestress force at each layers at the end of 2017 in kN
EP17_1=P1-(LP1+(0.0285*fc*(t17-1)*Psi+200*10^-6*Es/log10(t17+2)+log10(24*t17)*(fp/fpy-0.55)*fp/40)*Ap1),EP17_2=EP17_1
EP17_3=P3-(LP3+(0.0285*fc*(t17-1)*Psi+200*10^-6*Es/log10(t17+2)+log10(24*t17)*(fp/fpy-0.55)*fp/40)*Ap3)
EP17_4=P4-(LP4+(0.0285*fc*(t17-1)*Psi+200*10^-6*Es/log10(t17+2)+log10(24*t17)*(fp/fpy-0.55)*fp/40)*Ap4)
EP17_5=P5-(LP5+(0.0285*fc*(t17-1)*Psi+200*10^-6*Es/log10(t17+2)+log10(24*t17)*(fp/fpy-0.55)*fp/40)*Ap5),EP17_6=EP17_3
%Calculate cumulative upward deflection(camber) by EP in straight rebar in mm
Dup_17=L^2*(EP17_1*e1+EP17_2*e2+EP17_3*e3+EP17_4*e4+EP17_5*e5+EP17_6*e6)/(8*Ec*I)
%Calculate cumulative downward deflection by self-weight of girder, wearing surface and CESAL in mm
Ddown_17=5*L^3*(Pg+Pw+P17)/(384*Ec*I)

%Calculate net deflection in mm
Dnet_17=Dup_17-Ddown_17
%Deflection at the end of 2018
%calculate total effective prestress force at each layers at the end of 2018 in kN
EP18_1=P1-(LP1+(0.0285*fc*(t18-1)*Psi+200*10^-6*Es/log10(t18+2)+log10(24*t18)*(fp/fpy-0.55)*fp/40)*Ap1),EP18_2=EP18_1
EP18_3=P3-(LP3+(0.0285*fc*(t18-1)*Psi+200*10^-6*Es/log10(t18+2)+log10(24*t18)*(fp/fpy-0.55)*fp/40)*Ap3)
EP18_4=P4-(LP4+(0.0285*fc*(t18-1)*Psi+200*10^-6*Es/log10(t18+2)+log10(24*t18)*(fp/fpy-0.55)*fp/40)*Ap4)
EP18_5=P5-(LP5+(0.0285*fc*(t18-1)*Psi+200*10^-6*Es/log10(t18+2)+log10(24*t18)*(fp/fpy-0.55)*fp/40)*Ap5),EP18_6=EP18_3
%Calculate cumulative upward deflection (camber) by EP in straight rebar in mm
Dup_18=L^2*(EP18_1*e1+EP18_2*e2+EP18_3*e3+EP18_4*e4+EP18_5*e5+EP18_6*e6)/(8*Ec*I)
%Calculate cumulative downward deflection by self-weight of girder, wearing surface and CESAL in mm
Ddown_18=5*L^3*(Pg+Pw+P18)/(384*Ec*I)
%Calculate net deflection in mm
Dnet_18=Dup_18-Ddown_18

%Deflection at the end of 2019
%calculate total effective prestress force at each layers at the end of 2019 in kN
EP19_1=P1-(LP1+(0.0285*fc*(t19-1)*Psi+200*10^-6*Es/log10(t19+2)+log10(24*t19)*(fp/fpy-0.55)*fp/40)*Ap1),EP19_2=EP19_1
EP19_3=P3-(LP3+(0.0285*fc*(t19-1)*Psi+200*10^-6*Es/log10(t19+2)+log10(24*t19)*(fp/fpy-0.55)*fp/40)*Ap3)
EP19_4=P4-(LP4+(0.0285*fc*(t19-1)*Psi+200*10^-6*Es/log10(t19+2)+log10(24*t19)*(fp/fpy-0.55)*fp/40)*Ap4)
EP19_5=P5-(LP5+(0.0285*fc*(t19-1)*Psi+200*10^-6*Es/log10(t19+2)+log10(24*t19)*(fp/fpy-0.55)*fp/40)*Ap5),EP19_6=EP19_3
%Calculate cumulative upward deflection (camber) by EP in straight rebar in mm
Dup_19=L^2*(EP19_1*e1+EP19_2*e2+EP19_3*e3+EP19_4*e4+EP19_5*e5+EP19_6*e6)/(8*Ec*I)
%Calculate cumulative downward deflection by self-weight of girder, wearing surface and CESAL in mm
Ddown_19=5*L^3*(Pg+Pw+P19)/(384*Ec*I)
%Calculate net deflection in mm
Dnet_19=Dup_19-Ddown_19

%Deflection at the end of 2020
%calculate total effective prestress force at each layers at the end of 2020 in kN
EP20_1=P1-(LP1+(0.0285*fc*(t20-1)*Psi+200*10^-6*Es/log10(t20+2)+log10(24*t20)*(fp/fpy-0.55)*fp/40)*Ap1),EP20_2=EP20_1
EP20_3=P3-(LP3+(0.0285*fc*(t20-1)*Psi+200*10^-6*Es/log10(t20+2)+log10(24*t20)*(fp/fpy-0.55)*fp/40)*Ap3)
EP20_4=P4-(LP4+(0.0285*fc*(t20-1)*Psi+200*10^-6*Es/log10(t20+2)+log10(24*t20)*(fp/fpy-0.55)*fp/40)*Ap4)
EP20_5=P5-(LP5+(0.0285*fc*(t20-1)*Psi+200*10^-6*Es/log10(t20+2)+log10(24*t20)*(fp/fpy-0.55)*fp/40)*Ap5),EP20_6=EP20_3
%Calculate cumulative upward deflection (camber) by EP in straight rebar in mm
Dup_20=L^2*(EP20_1*e1+EP20_2*e2+EP20_3*e3+EP20_4*e4+EP20_5*e5+EP20_6*e6)/(8*Ec*I)
%Calculate cumulative downward deflection by self-weight of girder, wearing surface and CESAL in mm
Ddown_20=5*L^3*(Pg+Pw+P20)/(384*Ec*I)
%Calculate net deflection in mm
Dnet_20=Dup_20-Ddown_20

%Deflection at the end of 2021
%calculate total effective prestress force at each layers at the end of 2021 in kN

EP21_1=P1-(LP1+(0.0285*fc*(t21-1)*Psi+200*10^-6*Es/log10(t21+2)+log10(24*t21)*(fp/fpy-0.55)*fp/40)*Ap1),EP21_2=EP21_1

EP21_3=P3-(LP3+(0.0285*fc*(t21-1)*Psi+200*10^-6*Es/log10(t21+2)+log10(24*t21)*(fp/fpy-0.55)*fp/40)*Ap3)

EP21_4=P4-(LP4+(0.0285*fc*(t21-1)*Psi+200*10^-6*Es/log10(t21+2)+log10(24*t21)*(fp/fpy-0.55)*fp/40)*Ap4)

EP21_5=P5-(LP5+(0.0285*fc*(t21-1)*Psi+200*10^-6*Es/log10(t21+2)+log10(24*t21)*(fp/fpy-0.55)*fp/40)*Ap5),EP21_6=EP21_3

%Calculate cumulative upward deflection (camber) by EP in straight rebar in mm

Dup_21=L^2*(EP21_1*e1+EP21_2*e2+EP21_3*e3+EP21_4*e4+EP21_5*e5+EP21_6*e6)/(8*Ec*I)

%Calculate cumulative downward deflection by self-weight of girder, wearing surface and CESAL in mm

Ddown_21=5*L^3*(Pg+Pw+P21)/(384*Ec*I)

%Calculate net deflection in mm

Dnet_21=Dup_21-Ddown_21

%Deflection at the end of 2022

%calculate total effective prestress force at each layers at the end of 2022 in kN

EP22_1=P1-(LP1+(0.0285*fc*(t22-1)*Psi+200*10^-6*Es/log10(t22+2)+log10(24*t22)*(fp/fpy-0.55)*fp/40)*Ap1),EP22_2=EP22_1

EP22_3=P3-(LP3+(0.0285*fc*(t22-1)*Psi+200*10^-6*Es/log10(t22+2)+log10(24*t22)*(fp/fpy-0.55)*fp/40)*Ap3)

EP22_4=P4-(LP4+(0.0285*fc*(t22-1)*Psi+200*10^-6*Es/log10(t22+2)+log10(24*t22)*(fp/fpy-0.55)*fp/40)*Ap4)

EP22_5=P5-(LP5+(0.0285*fc*(t22-1)*Psi+200*10^-6*Es/log10(t22+2)+log10(24*t22)*(fp/fpy-0.55)*fp/40)*Ap5),EP22_6=EP22_3

%Calculate cumulative upward deflection (camber) by EP in straight rebar in mm

Dup_22=L^2*(EP22_1*e1+EP22_2*e2+EP22_3*e3+EP22_4*e4+EP22_5*e5+EP22_6*e6)/(8*Ec*I)

%Calculate cumulative downward deflection by self-weight of girder, wearing surface and CESAL in mm

Ddown_22=5*L^3*(Pg+Pw+P22)/(384*Ec*I)

%Calculate net deflection in mm

Dnet_22=Dup_22-Ddown_22

%Deflection at the end of 2023

%calculate total effective prestress force at each layers at the end of 2023 in kN

EP23_1=P1-(LP1+(0.0285*fc*(t23-1)*Psi+200*10^-6*Es/log10(t23+2)+log10(24*t23)*(fp/fpy-0.55)*fp/40)*Ap1),EP23_2=EP23_1

EP23_3=P3-(LP3+(0.0285*fc*(t23-1)*Psi+200*10^-6*Es/log10(t23+2)+log10(24*t23)*(fp/fpy-0.55)*fp/40)*Ap3)

EP23_4=P4-(LP4+(0.0285*fc*(t23-1)*Psi+200*10^-6*Es/log10(t23+2)+log10(24*t23)*(fp/fpy-0.55)*fp/40)*Ap4)

EP23_5=P5-(LP5+(0.0285*fc*(t23-1)*Psi+200*10^-6*Es/log10(t23+2)+log10(24*t23)*(fp/fpy-0.55)*fp/40)*Ap5),EP23_6=EP23_3

%Calculate cumulative upward deflection (camber) by EP in straight rebar in mm

Dup_23=L^2*(EP23_1*e1+EP23_2*e2+EP23_3*e3+EP23_4*e4+EP23_5*e5+EP23_6*e6)/(8*Ec*I)

%Calculate cumulative downward deflection by self-weight of girder, wearing surface and CESAL in mm

Ddown_23=5*L^3*(Pg+Pw+P23)/(384*Ec*I)

%Calculate net deflection in mm

Dnet_23=Dup_23-Ddown_23

%Deflection at the end of 2024

%calculate total effective prestress force at each layers at the end of 2024 in kN

EP24_1=P1-(LP1+(0.0285*fc*(t24-1)*Psi+200*10^-6*Es/log10(t24+2)+log10(24*t24)*(fp/fpy-0.55)*fp/40)*Ap1),EP24_2=EP24_1

EP24_3=P3-(LP3+(0.0285*fc*(t24-1)*Psi+200*10^-6*Es/log10(t24+2)+log10(24*t24)*(fp/fpy-0.55)*fp/40)*Ap3)

EP24_4=P4-(LP4+(0.0285*fc*(t24-1)*Psi+200*10^-6*Es/log10(t24+2)+log10(24*t24)*(fp/fpy-0.55)*fp/40)*Ap4)

EP24_5=P5-(LP5+(0.0285*fc*(t24-1)*Psi+200*10^-6*Es/log10(t24+2)+log10(24*t24)*(fp/fpy-0.55)*fp/40)*Ap5),EP24_6=EP24_3

%Calculate cumulative upward deflection (camber) by EP in straight rebar in mm

Dup_24=L^2*(EP24_1*e1+EP24_2*e2+EP24_3*e3+EP24_4*e4+EP24_5*e5+EP24_6*e6)/(8*Ec*I)

%Calculate cumulative downward deflection by self-weight of girder, wearing surface and CESAL in mm

Ddown_24=5*L^3*(Pg+Pw+P24)/(384*Ec*I)

%Calculate net deflection in mm

Dnet_24=Dup_24-Ddown_24

%Deflection at the end of 2025

%calculate total effective prestress force at each layers at the end of 2025 in kN

EP25_1=P1-(LP1+(0.0285*fc*(t25-1)*Psi+200*10^-6*Es/log10(t25+2)+log10(24*t25)*(fp/fpy-0.55)*fp/40)*Ap1),EP25_2=EP25_1

EP25_3=P3-(LP3+(0.0285*fc*(t25-1)*Psi+200*10^-6*Es/log10(t25+2)+log10(24*t25)*(fp/fpy-0.55)*fp/40)*Ap3)

EP25_4=P4-(LP4+(0.0285*fc*(t25-1)*Psi+200*10^-6*Es/log10(t25+2)+log10(24*t25)*(fp/fpy-0.55)*fp/40)*Ap4)

EP25_5=P5-(LP5+(0.0285*fc*(t25-1)*Psi+200*10^-6*Es/log10(t25+2)+log10(24*t25)*(fp/fpy-0.55)*fp/40)*Ap5),EP25_6=EP25_3

%Calculate cumulative upward deflection (camber) by EP in straight rebar in mm

Dup_25=L^2*(EP25_1*e1+EP25_2*e2+EP25_3*e3+EP25_4*e4+EP25_5*e5+EP25_6*e6)/(8*Ec*I)

%Calculate cumulative downward deflection by self-weight of girder, wearing surface and CESAL in mm

Ddown_25=5*L^3*(Pg+Pw+P25)/(384*Ec*I)

%Calculate net deflection in mm

Dnet_25=Dup_25-Ddown_25

%Deflection at the end of 2026

%calculate total effective prestress force at each layers at the end of 2026 in kN

EP26_1=P1-(LP1+(0.0285*fc*(t26-1)*Psi+200*10^-6*Es/log10(t26+2)+log10(24*t26)*(fp/fpy-0.55)*fp/40)*Ap1),EP26_2=EP26_1

EP26_3=P3-(LP3+(0.0285*fc*(t26-1)*Psi+200*10^-6*Es/log10(t26+2)+log10(24*t26)*(fp/fpy-0.55)*fp/40)*Ap3)

EP26_4=P4-(LP4+(0.0285*fc*(t26-1)*Psi+200*10^-6*Es/log10(t26+2)+log10(24*t26)*(fp/fpy-0.55)*fp/40)*Ap4)

EP26_5=P5-(LP5+(0.0285*fc*(t26-1)*Psi+200*10^-6*Es/log10(t26+2)+log10(24*t26)*(fp/fpy-0.55)*fp/40)*Ap5),EP26_6=EP26_3

%Calculate cumulative upward deflection (camber) by EP in straight rebar in mm

Dup_26=L^2*(EP26_1*e1+EP26_2*e2+EP26_3*e3+EP26_4*e4+EP26_5*e5+EP26_6*e6)/(8*Ec*I)

%Calculate cumulative downward deflection by self-weight of girder, wearing surface and CESAL in mm

Ddown_26=5*L^3*(Pg+Pw+P26)/(384*Ec*I)

%Calculate net deflection in mm

Dnet_26=Dup_26-Ddown_26

%Deflection at the end of 2027

%calculate total effective prestress force at each layers at the end of 2027 in kN

EP27_1=P1-(LP1+(0.0285*fc*(t27-1)*Psi+200*10^-6*Es/log10(t27+2)+log10(24*t27)*(fp/fpy-0.55)*fp/40)*Ap1),EP27_2=EP27_1

EP27_3=P3-(LP3+(0.0285*fc*(t27-1)*Psi+200*10^-6*Es/log10(t27+2)+log10(24*t27)*(fp/fpy-0.55)*fp/40)*Ap3)

EP27_4=P4-(LP4+(0.0285*fc*(t27-1)*Psi+200*10^-6*Es/log10(t27+2)+log10(24*t27)*(fp/fpy-0.55)*fp/40)*Ap4)

EP27_5=P5-(LP5+(0.0285*fc*(t27-1)*Psi+200*10^-6*Es/log10(t27+2)+log10(24*t27)*(fp/fpy-0.55)*fp/40)*Ap5),EP27_6=EP27_3

%Calculate cumulative upward deflection (camber) by EP in straight rebar in mm

Dup_27=L^2*(EP27_1*e1+EP27_2*e2+EP27_3*e3+EP27_4*e4+EP27_5*e5+EP27_6*e6)/(8*Ec*I)
%Calculate cumulative downward deflection by self-weight of girder, wearing surface and CESAL in mm
Ddown_27=5*L^3*(Pg+Pw+P27)/(384*Ec*I)
%Calculate net deflection in mm
Dnet_27=Dup_27-Ddown_27
%Deflection at the end of 2028
%calculate total effective prestress force at each layers at the end of 2028 in kN
EP28_1=P1-(LP1+(0.0285*fc*(t28-1)*Psi+200*10^-6*Es/log10(t28+2)+log10(24*t28)*(fp/fpy-0.55)*fp/40)*Ap1),EP28_2=EP28_1
EP28_3=P3-(LP3+(0.0285*fc*(t28-1)*Psi+200*10^-6*Es/log10(t28+2)+log10(24*t28)*(fp/fpy-0.55)*fp/40)*Ap3)
EP28_4=P4-(LP4+(0.0285*fc*(t28-1)*Psi+200*10^-6*Es/log10(t28+2)+log10(24*t28)*(fp/fpy-0.55)*fp/40)*Ap4)
EP28_5=P5-(LP5+(0.0285*fc*(t28-1)*Psi+200*10^-6*Es/log10(t28+2)+log10(24*t28)*(fp/fpy-0.55)*fp/40)*Ap5),EP28_6=EP28_3
%Calculate cumulative upward deflection (camber) by EP in straight rebar in mm
Dup_28=L^2*(EP28_1*e1+EP28_2*e2+EP28_3*e3+EP28_4*e4+EP28_5*e5+EP28_6*e6)/(8*Ec*I)
%Calculate cumulative downward deflection by self-weight of girder, wearing surface and CESAL in mm
Ddown_28=5*L^3*(Pg+Pw+P28)/(384*Ec*I)
%Calculate net deflection in mm
Dnet_28=Dup_28-Ddown_28
%Deflection at the end of 2029
%calculate total effective prestress force at each layers at the end of 2029 in kN
EP29_1=P1-(LP1+(0.0285*fc*(t29-1)*Psi+200*10^-6*Es/log10(t29+2)+log10(24*t29)*(fp/fpy-0.55)*fp/40)*Ap1),EP29_2=EP29_1
EP29_3=P3-(LP3+(0.0285*fc*(t29-1)*Psi+200*10^-6*Es/log10(t29+2)+log10(24*t29)*(fp/fpy-0.55)*fp/40)*Ap3)
EP29_4=P4-(LP4+(0.0285*fc*(t29-1)*Psi+200*10^-6*Es/log10(t29+2)+log10(24*t29)*(fp/fpy-0.55)*fp/40)*Ap4)
EP29_5=P5-(LP5+(0.0285*fc*(t29-1)*Psi+200*10^-6*Es/log10(t29+2)+log10(24*t29)*(fp/fpy-0.55)*fp/40)*Ap5),EP29_6=EP29_3
%Calculate cumulative upward deflection (camber) by EP in straight rebar in mm
Dup_29=L^2*(EP29_1*e1+EP29_2*e2+EP29_3*e3+EP29_4*e4+EP29_5*e5+EP29_6*e6)/(8*Ec*I)
%Calculate cumulative downward deflection by self-weight of girder, wearing surface and CESAL in mm
Ddown_29=5*L^3*(Pg+Pw+P29)/(384*Ec*I)
%Calculate net deflection in mm
Dnet_29=Dup_29-Ddown_29
%Deflection at the end of 2030
%calculate total effective prestress force at each layers at the end of 2030 in kN
EP30_1=P1-(LP1+(0.0285*fc*(t30-1)*Psi+200*10^-6*Es/log10(t30+2)+log10(24*t30)*(fp/fpy-0.55)*fp/40)*Ap1),EP30_2=EP30_1
EP30_3=P3-(LP3+(0.0285*fc*(t30-1)*Psi+200*10^-6*Es/log10(t30+2)+log10(24*t30)*(fp/fpy-0.55)*fp/40)*Ap3)
EP30_4=P4-(LP4+(0.0285*fc*(t30-1)*Psi+200*10^-6*Es/log10(t30+2)+log10(24*t30)*(fp/fpy-0.55)*fp/40)*Ap4)
EP30_5=P5-(LP5+(0.0285*fc*(t30-1)*Psi+200*10^-6*Es/log10(t30+2)+log10(24*t30)*(fp/fpy-0.55)*fp/40)*Ap5),EP30_6=EP30_3
%Calculate cumulative upward deflection (camber) by EP in straight rebar in mm
Dup_30=L^2*(EP30_1*e1+EP30_2*e2+EP30_3*e3+EP30_4*e4+EP30_5*e5+EP30_6*e6)/(8*Ec*I)
%Calculate cumulative downward deflection by self-weight of girder, wearing surface and CESAL in mm
Ddown_30=5*L^3*(Pg+Pw+P30)/(384*Ec*I)
%Calculate net deflection in mm
Dnet_30=Dup_30-Ddown_30
%THE END%

Appendix 2 MATLAB output

t14 =30	As6 =283.5287	Alpha2 =0	EPt4 =3.7071e+005
t15 =395	Ap1 =1.3672e+004	Alpha3 =0	EPt5 =1.1121e+006
t16 =760	Ap2 =1.3672e+004	Alpha4 = 0	EPt6 =1.2238e+006
t17 =1125	Ap3 = 1.9280e+004	Alpha5 =0	EPt =5.6661e+006
t18 =1490	Ap4 =5.8402e+003	Alpha6 =0	EP14_1 = 7.7749e+005
t19 =1855	Ap5 =1.7521e+004	Alpha =6.6667	EP14_2 =7.7749e+005
t20 =2220	Ap6 =1.9280e+004	fc =11.0225	EP14_3 =1.0964e+006
t21 =2585	Ap = 8.9265e+004	x =35000	EP14_4 =3.3211e+005
t22 =2950	fpy =313.0470	Esh =73.4833	EP14_5 =9.9633e+005
t23 =3315	fp =260.8725	Fr = 82.1748	EP14_6 = 1.0964e+006
t24 =3680	P1 =3.5667e+006	Asl =15	Dup_14 =28.9050
t25 =4045	P2 =3.5667e+006	IPL =170.6581	Ddown_14 =3.4048
t26 =4410	P3 = 5.0296e+006	LP1 = 2.3333e+006	Dnet_14 =25.5002
t27 =4775	P4 =1.5236e+006	LP2 = 2.3333e+006	EP15_1 =8.8154e+005
t28 =5140	P5 =4.5707e+006	LP3 =3.2903e+006	EP15_2 =8.8154e+005
t29 =5505	P6 =5.0296e+006	LP4 =9.9668e+005	EP15_3 =1.2431e+006
t30 =5870	P =2.3287e+007	LP5 =2.9900e+006	EP15_4 =3.7656e+005
Ac =4038000	Pg =7.0665e+003	LP6 = 3.2903e+006	EP15_5 =1.1297e+006
Yc =1.0251e+003	Pw = 415.8000	LPin = 1.5234e+007	EP15_6 =1.2431e+006
I1 =1.1008e+012	Y =304.6537	CR =4.2918	Dup_15 =32.7733
I2 =1.0683e+011	ep =720.4652	SR =14.5734	Ddown_15 =4.8100
I3 =1.0683e+011	e1 = 991.1189	RE =7.8737	Dnet_15 =27.9634
I4 =1.0638e+012	e2 =809.1189	LPLt =26.7390	EP16_1 =8.6785e+005
I =2.3783e+012	e3 =515.1189	LPt =2.3869e+006	EP16_2 =8.6785e+005
As1 = 201.0619	e4 =939.8811	TPLt =197.3971	EP16_3 = 1.2238e+006
As2 =201.0619	e5 =729.8811	TLPt =1.7621e+007	EP16_4 =3.7071e+005
As3 =283.5287	e6 =484.8811	EPt1 = 8.6785e+005	EP16_5 =1.1121e+006
As4 =132.7323	yb =745.0000	EPt2 =8.6785e+005	EP16_6 =1.2238e+006
As5 =132.7323	Alpha1 =0	EPt3 =1.2238e+006	Dup_16 =32.2644

Ddown_16 =5.1682

Dnet_16 =27.0962

EP17_1 =8.4642e+005

EP17_2 =8.4642e+005

EP17_3 =1.1936e+006

EP17_4 =3.6156e+005

EP17_5 =1.0847e+006

EP17_6 =1.1936e+006

Dup_17 =31.4679

Ddown_17 =5.5271

Dnet_17 =25.9408

EP18_1 =8.2235e+005

EP18_2 =8.2235e+005

EP18_3 =1.1596e+006

EP18_4 =3.5127e+005

EP18_5 =1.0538e+006

EP18_6 =1.1596e+006

Dup_18 =30.5728

Ddown_18 =5.9128

Dnet_18 =24.6599

EP19_1 =7.9699e+005

EP19_2 =7.9699e+005

EP19_3 =1.1239e+006

EP19_4 =3.4044e+005

EP19_5 =1.0213e+006

EP19_6 =1.1239e+006

Dup_19 =29.6299

Ddown_19 =6.3278

Dnet_19 =23.3021

EP20_1 =7.7089e+005

EP20_2 =7.7089e+005

EP20_3 =1.0871e+006

EP20_4 =3.2929e+005

EP20_5 =9.8788e+005

EP20_6 =1.0871e+006

Dup_20 =28.6596

Ddown_20 =6.7749

Dnet_20 =21.8847

EP21_1 =7.4432e+005

EP21_2 =7.4432e+005

EP21_3 =1.0496e+006

EP21_4 =3.1794e+005

EP21_5 =9.5383e+005

EP21_6 =1.0496e+006

Dup_21 =27.6719

Ddown_21 =7.2554

Dnet_21 =20.4165

EP22_1 =7.1743e+005

EP22_2 =7.1743e+005

EP22_3 =1.0117e+006

EP22_4 =3.0646e+005

EP22_5 =9.1937e+005

EP22_6 =1.0117e+006

Dup_22 =26.6723

Ddown_22 =3.9670

Dnet_22 =22.7053

EP23_1 =6.9031e+005

EP23_2 =6.9031e+005

EP23_3 =9.7345e+005

EP23_4 =2.9487e+005

EP23_5 =8.8462e+005

EP23_6 =9.7345e+005

Dup_23 =25.6641

Ddown_23 =4.1363

Dnet_23 =21.5278

EP24_1 =6.6302e+005

EP24_2 =6.6302e+005

EP24_3 =9.3496e+005

EP24_4 =2.8322e+005

EP24_5 =8.4965e+005

EP24_6 =9.3496e+005

Dup_24 =24.6495

Ddown_24 =4.3062

Dnet_24 =20.3433

EP25_1 =6.3560e+005

EP25_2 = 6.3560e+005

EP25_3 =8.9629e+005

EP25_4 =2.7150e+005

EP25_5 =8.1451e+005

EP25_6 =8.9629e+005

Dup_25 =23.6299

Ddown_25 =4.4833

Dnet_25 =19.1467

EP26_1 =6.0807e+005

EP26_2 =6.0807e+005

EP26_3 =8.5747e+005

EP26_4 =2.5974e+005

EP26_5 =7.7923e+005

EP26_6 =8.5747e+005

Dup_26 =22.6065

Ddown_26 = 4.6693

Dnet_26 =17.9373

EP27_1 =5.8046e+005

EP27_2 =5.8046e+005

EP27_3 =8.1854e+005

EP27_4 =2.4795e+005

EP27_5 =7.4385e+005

EP27_6 =8.1854e+005

Dup_27 =21.5800

Ddown_27 =4.8630

Dnet_27 =16.7170

EP28_1 =5.5278e+005

EP28_2 = 5.5278e+005

EP28_3 =7.7950e+005

EP28_4 =2.3612e+005

EP28_5 =7.0837e+005

EP28_6 =7.7950e+005

Dup_28 =20.5508

Ddown_28 =5.0663

Dnet_28 =15.4845

EP29_1 =5.2504e+005

EP29_2 =5.2504e+005

EP29_3 =7.4039e+005

EP29_4 =2.2428e+005

EP29_5 =6.7283e+005

EP29_6 =7.4039e+005

Dup_29 =19.5196

Ddown_29 =5.2785

Dnet_29 =14.2410

EP30_1 =4.9725e+005

EP30_2 =4.9725e+005

EP30_3 =7.0120e+005   EP30_4 =2.1241e+005

    EP30_5 =6.3722e+005   EP30_6 =7.0120e+005

        Dup_30 =18.4865   Ddown_30 =5.5003

    == THE END==   Dnet_30 =12.9862

Appendix 4 List of drawings

DETAIL OF WATERPROOFING